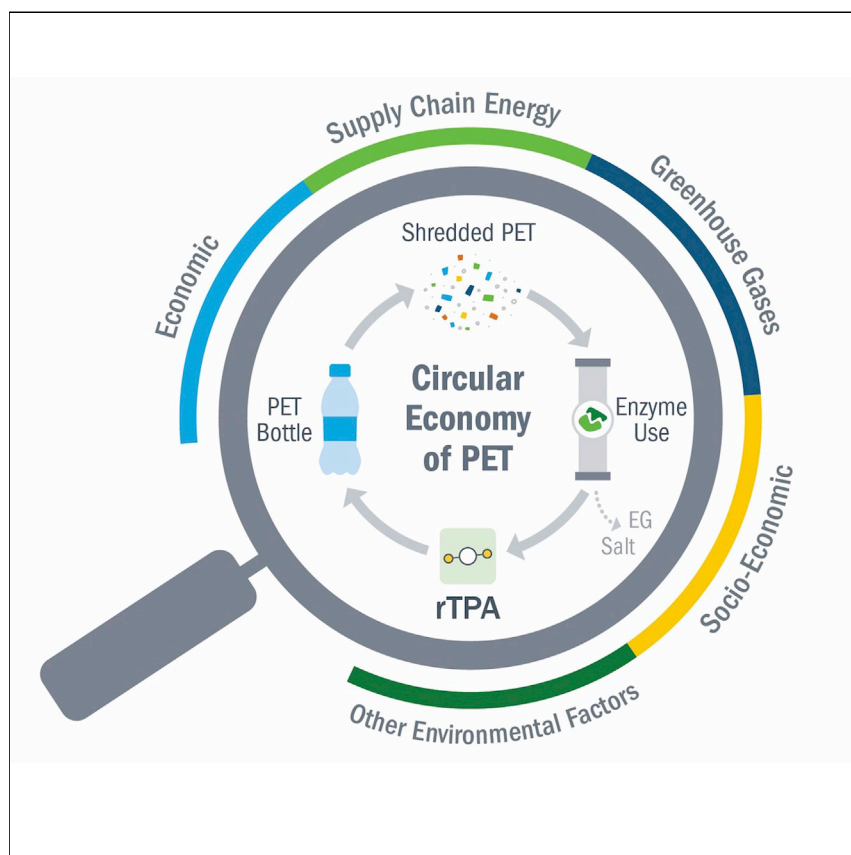


Article

Techno-economic, life-cycle, and socioeconomic impact analysis of enzymatic recycling of poly(ethylene terephthalate)



Avantika Singh, Nicholas A. Rorrer, Scott R. Nicholson, ..., Alberta C. Carpenter, John E. McGeehan, Gregg T. Beckham

gregg.beckham@nrel.gov

Highlights

Enzymes expand PET-recycling options beyond chemo-catalytic and thermal methods

Process analyses reveal key economic drivers for enzymatic PET recycling

Enzymatic PET recycling can be cost-competitive with virgin PET manufacturing costs

Circularity of the PET economy offers sustainability and socioeconomic benefits

This study presents a comprehensive process, economic, environmental, and socioeconomic analysis of the enzymatic recycling of poly(ethylene terephthalate), which is the most widely used synthetic polyester. The analyses predict that PET deconstruction using enzymes can achieve cost parity with terephthalic acid manufacturing as well as substantial reductions in both supply chain energy use and greenhouse gas emissions relative to virgin polyester manufacturing. This study also highlights key research areas for further impactful development of biocatalysis-enabled plastics recycling.

Singh et al., *Joule* 5, 2479–2503
September 15, 2021 © 2021 The Author(s).
Published by Elsevier Inc.
<https://doi.org/10.1016/j.joule.2021.06.015>



Article

Techno-economic, life-cycle, and socioeconomic impact analysis of enzymatic recycling of poly(ethylene terephthalate)

Avantika Singh,^{1,2} Nicholas A. Rorrer,^{1,3} Scott R. Nicholson,^{1,4} Erika Erickson,^{1,3} Jason S. DesVeaux,^{1,2} Andre F.T. Avelino,⁴ Patrick Lamers,⁴ Arpit Bhatt,⁴ Yimin Zhang,⁴ Greg Avery,⁴ Ling Tao,² Andrew R. Pickford,^{1,5} Alberta C. Carpenter,^{1,4} John E. McGeehan,^{1,5} and Gregg T. Beckham^{1,3,6,*}

SUMMARY

Esterases have emerged as important biocatalysts for enzyme-based polyester recycling of poly(ethylene terephthalate) (PET) to terephthalic acid (TPA) and ethylene glycol (EG). Here, we present process modeling, techno-economic, life-cycle, and socioeconomic impact analyses for an enzymatic PET depolymerization-based recycling process, which we compare with virgin TPA manufacturing. We predict that enzymatically recycled TPA (rTPA) can be cost-competitive and highlight key areas to achieve this. In addition to favorable long-term socioeconomic benefits, rTPA can reduce total supply chain energy use by 69%–83% and greenhouse gas emissions by 17%–43% per kg of TPA. An economy-wide assessment for the US estimates that the TPA recycling process can reduce environmental impacts by up to 95% while generating up to 45% more socioeconomic benefits, also relative to virgin TPA production. Sensitivity analyses highlight impactful research opportunities to pursue toward realizing biological PET recycling and upcycling.

INTRODUCTION

Despite widespread application in daily life, there are limited options for the recycling of synthetic plastics, which presents an opportunity for the development of critical new technologies. As plastics accumulate both in landfills and in the natural environment, these materials are causing a global pollution crisis due to their recalcitrance against abiotic and biological breakdown.^{1–3} Compounding the issue, the current mechanical recycling industry often produces lower-value products and is unable to recycle many types of plastics. This confluence of environmental concerns and the limitations of current recycling technology have catalyzed renewed interest from the global research and industrial communities to pursue recycling strategies that rely on depolymerization of polymers into their constituent monomers or other processable, non-polymeric intermediates, namely via chemical recycling.⁴

Poly(ethylene terephthalate) (PET) is the most abundantly produced synthetic polyester in circulation today,^{1,5} produced globally at 82 million metric tons (MMT) per year.⁶ The majority (54%) of PET is used in the production of textiles and fibers, with 24 MMT (or 29%) undergoing further polymerization to produce resin for rigid containers and single-use bottles, whereas the rest is used in films and other applications.⁷ Looking at the PET consumed annually in the United States (US),⁵ which is approximately 3 MMT, only 18.5% is currently processed by mechanical recyclers.⁸

Context & scale

Chemical recycling and upcycling of plastics will be critical technologies to address the plastic pollution challenge. Given multiple process options for recycling plastics, rigorous process analysis is necessary to identify challenges that must be overcome for a technology to reach an industrial scale. For PET recycling, several chemical recycling strategies have been proposed and, in some cases—chemo-catalytic and thermal approaches—are being scaled up. Given that PET exhibits labile ester bonds that are also common in natural biological systems, the research community is vigorously pursuing the engineering of esterase enzymes to depolymerize PET. This study applies process analysis to highlight drivers that the community can focus on to accelerate the development of a biological PET depolymerization process and also provides a basis to compare current and future enzyme-based approaches for PET-recycling to chemo-catalytic and thermal methods.



Therefore, to achieve higher rates of PET recycling and potentially include PET substrates such as textiles that are not currently recycled, multiple chemical recycling strategies for PET have been proposed, developed, and, in some cases, scaled up over the last several decades.^{4,9,10} Methanolysis, hydrolysis, aminolysis, glycolysis, and thermal depolymerization strategies are among the most well-studied chemical recycling processes for PET.^{4,9,10}

PET is synthesized mainly via polycondensation of two building blocks: terephthalic acid (TPA) and ethylene glycol (EG). The inter-monomer chemical linkage in PET is an ester bond, which is a prevalent linkage in biomolecules. For example, cutin, suberin, hemicellulose, and lignin are abundant plant-derived polymers, all of which exhibit ester bonds.^{11–13} Given the prevalence of aromatic and aliphatic building blocks in ester-linked natural polymers, it is perhaps not surprising, in hindsight, that esterase enzymes can cleave ester bonds in PET and other synthetic polyesters.^{14–19} Considering the potential for esterases to deconstruct PET under mild conditions, the global research community is vigorously pursuing efforts in prospecting for new PET-degrading enzymes (PET hydrolases), solving crystal structures thereof, and engineering and evolving these enzymes for improved PET degradation capacity, with the aim of developing efficient biocatalysts for use as a chemical recycling approach to address this common polyester.^{20–36}

Given the growth in research related to biocatalyst development for PET depolymerization, it is critical to understand the projected economic and sustainability impacts that such a process could have toward enabling PET circularity. To that end, we present here a rigorous, comprehensive modeling effort for a conceptual enzymatic process to depolymerize PET to recycled TPA (rTPA) and EG, including all utilities required for an integrated process. Techno-economic analysis (TEA) of this process enables predictions of the capital and operating costs to project the minimum selling price (MSP) for rTPA, including the sale of the two co-products, EG and sodium sulfate (SS). Sensitivity analyses are employed to highlight the importance of the biocatalytic rate, enzyme loading, and enzyme cost, along with multiple additional, tunable process variables that are important for further process improvement and optimization. We employ the Materials Flow through Industry (MFI) tool³⁷ to estimate the total supply chain energy and greenhouse gas (GHG) emissions for rTPA production from reclaimed PET via this enzyme-based PET deconstruction process and compare this with virgin TPA (vTPA) production. We expand this MFI analysis to include the use of a top-down, environmentally extended input-output (EEIO) model³⁸ to evaluate the US economy-wide impacts of implementing the rTPA process and compare it with the production of vTPA across multiple environmental and socioeconomic indexes.

Taken together, the results in this study highlight the most crucial process steps to improve enzyme-based recycling technologies for PET. In addition to the economic factors, this work identifies important sustainability drivers for realizing environmental benefits (i.e., reduced resource use and byproduct release) and socioeconomic potential (i.e., added economic value and number of jobs) possible through an enzyme-based PET-recycling strategy.

Process and economic model construction

A process model for enzymatic PET depolymerization was developed by Aspen Plus to explore how the assumptions and process requirements impact the process economics and sustainability. Figure 1 presents a simplified process flow diagram (PFD) for the base case, whereas a detailed PFD indicating all model inputs is provided in Figures S1–S4. The recycling facility is modeled on the scale of 150 Mt of PET flakes processed per day

¹BOTTLE Consortium, Golden, CO 80401, USA

²Catalytic Carbon Transformation and Scale-Up Center, National Renewable Energy Laboratory, Golden, CO 80401, USA

³Renewable Resources and Enabling Sciences Center, National Renewable Energy Laboratory, Golden, CO 80401, USA

⁴Strategic Energy Analysis Center, National Renewable Energy Laboratory, Golden, CO 80401, USA

⁵Centre for Enzyme Innovation, University of Portsmouth, Portsmouth PO1 2DY, UK

⁶Lead contact

*Correspondence: gregg.beckham@nrel.gov
<https://doi.org/10.1016/j.joule.2021.06.015>

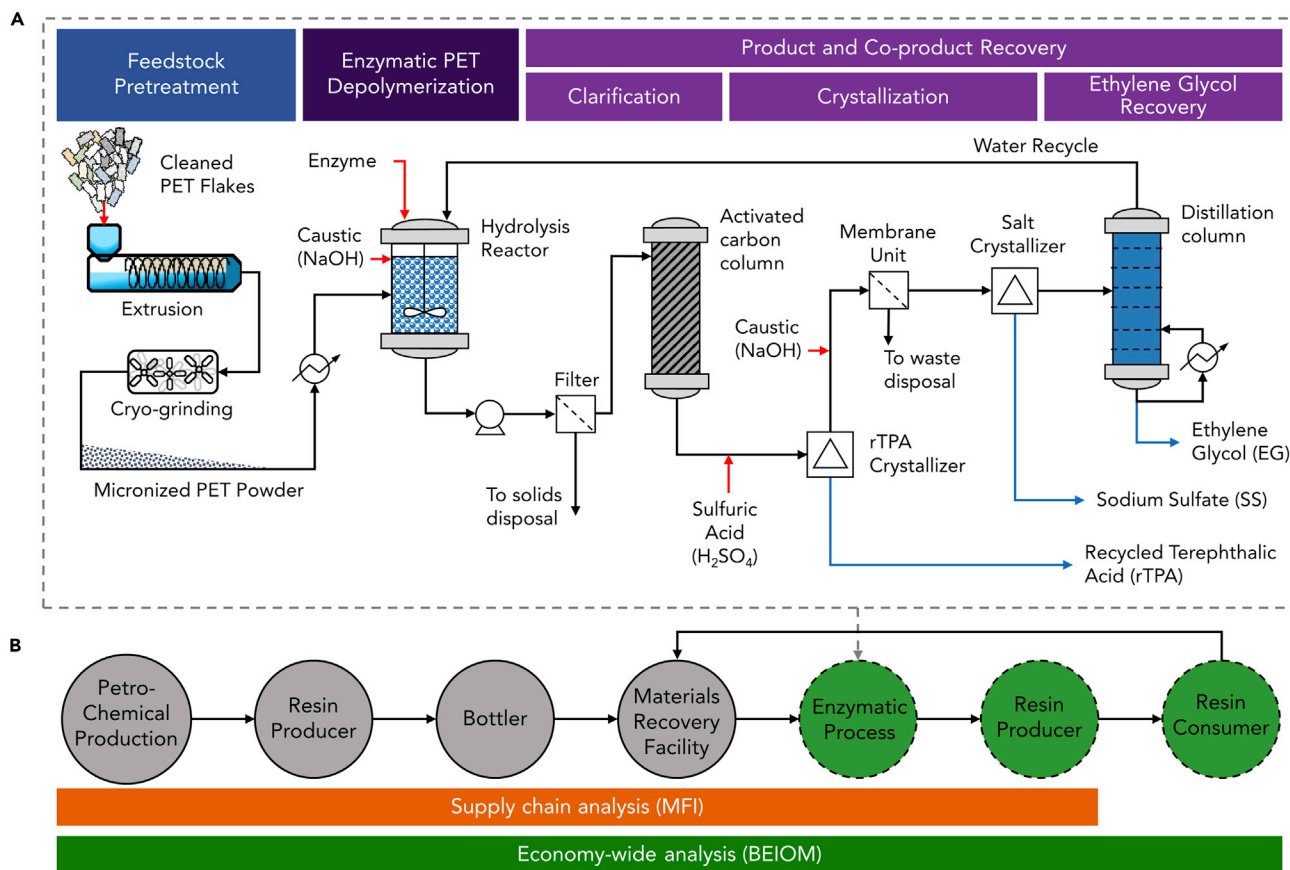


Figure 1. Enzymatic PET-recycling process design and representation of supply chain and economy-wide analysis

(A) Simplified process flow diagram of the PET enzymatic depolymerization process, divided into three sections. In the first section, polyester flakes are pre-treated (e.g., extrusion, size reduction, etc.) and subsequently enzymatically depolymerized in the second section. Following depolymerization, rTPA, SS (salt), and EG are recovered via downstream processes in the third section. PET flakes and other raw material inputs are shown in red, intermediate, recycle, and waste streams are shown in black, and the product and co-product streams are shown in blue. Case studies were performed to evaluate key variables and process operations in each process section, labeled at the top of the upper panel.

(B) A representation of the supply chain modeled for the bottom-up MFI tool assessment in orange, and the top-down life cycle assessment by the BEIOM tool in green. BEIOM considers the supply chain for the production of rTPA, as well as production, distribution use, and environmental and socioeconomic factors. The detailed process flow diagram of the base case design as modeled in Aspen Plus is presented in [Figures S1–S4](#).

(~50,000 Mt/year). For reference, the average annual capacity of a US PET production plant is 88,000 Mt/year.⁶ The plant size modeled here represents 1.7% of all PET currently consumed in the US and 7% of the PET volume currently recycled in the US. Post-consumer PET recycling in the US is primarily conducted for single-use beverage bottles and, in total, accounts for ~0.68 MMT (1,503 million pounds) of PET per year, which is ~29% of all PET bottles consumed annually in the US.³⁹ The modeled facility is assumed to be in close proximity to another manufacturing plant, such as a PET polymerization plant or a petroleum refinery, such that high-pressure steam, cooling water, and wastewater treatment are assumed to be over-the-fence and priced accordingly as utility operating expenses. Capital investment to build the auxiliary infrastructure for utilities is accounted in the outside battery limit costs.

In the baseline case, we assume that clean PET flakes, consisting of approximately 30% colored flakes, are obtained directly from a recycler, priced at \$0.66/kg.^{40,41} The recyclable fraction (i.e., PET fraction, denoted by Φ) of the total feed is assumed to be 0.95, with the remainder being contaminants such as caps, labels, adhesives,

dirt, etc. Although enzymatic recycling is of potentially greater significance for dirty, comingled streams, we had access to more reliable data on market prices of clean PET flakes. Hence, the base case considered clean, colored flakes, which serves as a conservative projection of the rTPA price. Other scenarios with different PET feedstock prices and PET purity are analyzed as sensitivity cases. Prior to depolymerization, feedstock pretreatment steps designed to improve enzymatic conversion are modeled in which clean PET flakes are fed to an extruder that heats the plastic above its melting point ($T_m \sim 260^\circ\text{C}$). The molten PET is then quenched to yield PET with lower crystallinity, followed by size reduction via a microgranulator.⁴² This series of pretreatment steps results in a PET powder with particle sizes of less than 1 mm prior to enzymatic depolymerization, in line with recent literature.^{35,42} Unlike mechanical recycling, drying is not required in this sequence.

Following mechanical pretreatment, the plastic is fed to a series of stirred-tank reactors for depolymerization to rTPA and EG via enzymatic hydrolysis. Specifically, the PET stream is conveyed to a series of stirred tanks (950 m³ vessels) with a modeled solids loading of 15% in the base case.³⁵ The depolymerization process is catalyzed by a generalized PET hydrolase that is produced offsite and purchased directly for use in this process. Products of PET hydrolysis are recovered in this process scheme upon reaching a 90% PET degradation extent.³⁵ Additionally, this model ignores other monomers that may be present in PET (e.g., isophthalic acid, 1,4-cyclohexanediol, diethylene glycol, etc.).

After enzymatic depolymerization, the hydrolysate is passed through a filter press where the remaining solids are separated from the reaction solution, followed by ultrafiltration to remove the enzymes. The filtrate is subsequently passed through an activated carbon column to remove additives such as dyes and pigments.^{35,43,44} These steps inherently assume that rTPA at pH > 7 remains soluble in the aqueous phase. The solution is then acidified by the addition of sulfuric acid to lower the pH to 2.5 and cooled to precipitate rTPA.^{44,45} The precipitate is passed through a continuous crystallizer and dried to recover rTPA crystals at a purity of >98%.^{44,46} The remaining liquor is neutralized to pH 7 by the addition of caustic (e.g., NaOH) and passed through a membrane unit with 96.5% rejection for SS and 72% rejection for EG.^{47–49} The permeate, which is predominately water, is sent to the adjacent wastewater treatment, and the retentate is sent to a continuous crystallizer for SS recovery. The SS is assumed to be crystallized as Glauber's salt (the most stable hydrate form) with 98.5% purity and sold at a market price of \$0.15/kg⁵⁰ as a co-product (overall, 76% mass recovery, adjusted for anhydrous form). The model assumes that any remaining SS salt is lost during the processing steps, such that the mother liquor from salt crystallization primarily consists of EG and water. EG is subsequently recovered via a series of distillation columns to obtain EG at a purity of 99%, enabling it to be sold at market price (\$0.96/kg).⁵⁰ The overall recovery of rTPA and EG in the process is modeled at 90% and 50%, respectively, and these values are varied as parameters in the sensitivity analysis.

Material and energy balances from the model were used to estimate the required equipment size and capital investment, whereas information on raw materials, utilities, etc., was used to estimate the variable operating expenses. A discounted cash flow analysis approach with certain financial parameters (see [Table S1](#)) was applied to project the rTPA MSP produced by this facility, with EG and SS salt sold at their respective market prices as co-products. A summary of the results from this economic analysis can be found in [Table S2](#).

RESULTS

Base case scenario

The base case scenario, as outlined earlier, is a 150-metric-tons-per-day (MTPD)-sized plant that considers depolymerization of clean PET flakes ($\Phi = 0.95$, cost = \$0.66/kg, 30% color) to yield rTPA as a primary product, while EG (50% recovery, selling price \$0.96/kg) and SS (76% recovery, selling price \$0.15/kg) are sold as co-products. Co-product selling prices are based on a 5-year average of historical prices in the US. For reference, historic prices for vTPA and the co-products are provided in [Figures 2A](#) and [2B](#). Including revenue from co-products, rTPA achieves an MSP of \$1.93/kg with a majority of the cost attributed to the feedstock supply, shown in blue in the simplified cost breakdown chart ([Figure 2C](#)). The base case results for rTPA MSP can be further delineated by the process sections. The detailed MSP cost breakdown that combines the capital and operating contributions from each process step is shown in [Figure 2D](#).

The total capital investment for a plant designed to process 150 MTPD of PET flakes is projected to be ~\$67M ([Figure 2E](#)). The highest contribution (29%) to the total capital investment for constructing this plant is from product recovery steps, i.e., rTPA crystallization, salt recovery, and EG distillation, primarily owing to continuous crystallizers and distillation columns. Feedstock pretreatment, which consists of extrusion and cryo-micronization, and the depolymerization section, which consists of a series of batch hydrolysis reactors, contribute nearly equally to the capital expenses, at 20% each. Additionally, a 25% contribution is assumed from the outside battery limit (OSBL) investment, which consists of additional capital expenditure, such as development of piping, instrumentation, etc., required to integrate the over-the-fence utilities into the plant. Detailed information on the specific unit operations and the capital requirements for each process section is shown in [Table S3](#).

In addition to the initial capital expenditures, the plant will require \$44M per year in operating costs. As shown in [Figure 2F](#), these operating expenses are dominated by the feedstock cost, which is priced for clean PET flakes (containing 30% colored flakes) sourced from bottle recyclers.^{40,41} Electricity consumption is the other major driver in the pretreatment section, primarily required for melt extrusion and micro-grinding. In other process areas, the cost of chemicals such as caustic for pH maintenance, particularly in hydrolysis reactors, and sulfuric acid for rTPA crystallization are primary drivers. The cost contributions for these chemicals are largely offset by the recovery of SS, and salt recovery is being explored as a variation in the base case process design (*vide infra*). Similarly, steam usage in the distillation step is attributed to the EG recovery, which requires substantial water evaporation. In addition, maintenance costs for filter, activated carbon bed, and membrane replacement are accounted for in the economics. Further details of the operating costs are described in [Table S4](#).

Additional analysis, conducted by the MFI tool, estimates that rTPA has a 69% lower supply chain energy requirement ([Figure 2G](#)) and produces 17% less GHG ([Figure 2H](#)) than vTPA production. As shown in [Figure 1](#), we divide the base case into three sections: (1) feedstock pretreatment, (2) enzymatic PET depolymerization, and (3) product and co-product recovery (rTPA, EG, and SS).

To further examine the process sections, we considered three primary case studies focusing on variables within each section. In doing so, this work highlights the potential for further research and development across multiple disciplines and highlights

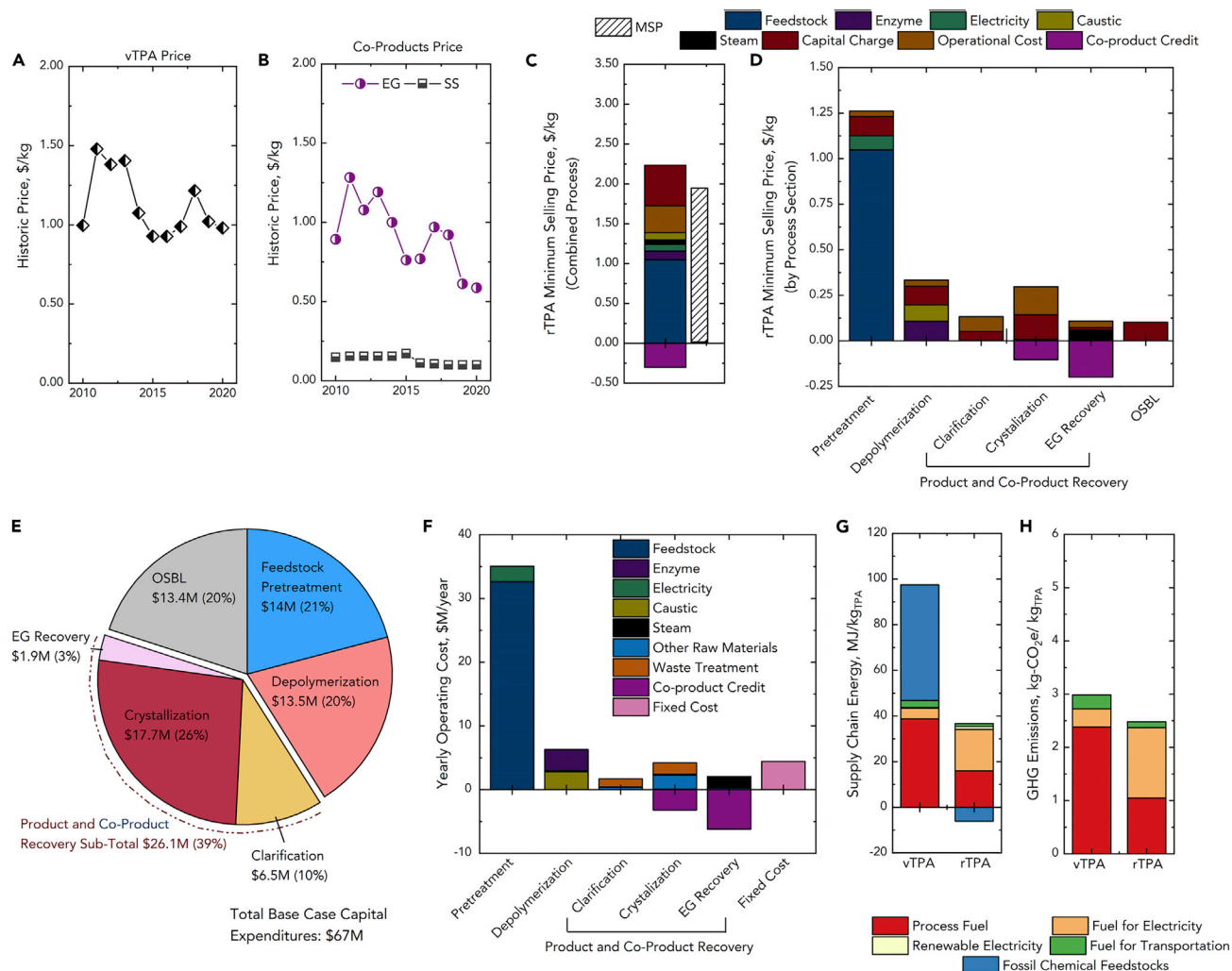


Figure 2. Detailed cost breakdown of rTPA in the base case

(A and B) The US historic price data for (A) vTPA and (B) the co-products (EG and SS).

(C and D) The summary of the base case results for the (C) minimum selling price from the combined process, (D) minimum selling price, both the capital and operating contributions, shown across each process section.

(E) Total capital investment of \$67M in the base case split into different steps of the recycling process, including outside battery limit (OSBL), which is assumed to be 25% of battery limit investment.

(F) Annual operating expenses for the proposed PET-recycling design, disaggregated by process step (total = \$44M/year). Raw materials include PET feedstock cost as well as other chemicals such as enzymes, caustic, and sulfuric acid, and co-products are EG and SS.

(G and H) The base case (G) supply chain energy, and (H) GHG emissions of rTPA are shown in comparison with vTPA. Numerical data in this figure are reported in Tables S5–S10.

the most important factors to be overcome to enable the commercial success of this technology.

Case study I: Feedstock pretreatment

In order to understand the opportunities for process improvement, we examined various parameters. As noted in the base case, feedstock cost is one of the largest contributors to rTPA MSP. Most feedstock costs are associated with the cleaning of PET bales and shredding into flakes.⁴¹ Due to the variable nature of post-consumer waste composition, and the lack of uniformity in sorting schemes, the purity grade and relative contaminant percentages of PET bales vary between material recovery facilities

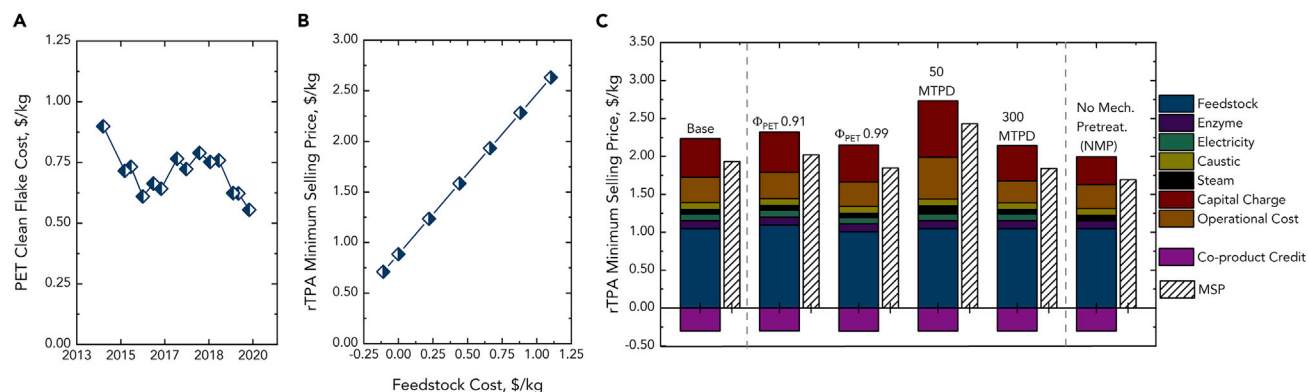


Figure 3. TEA sensitivity results for process parameters associated with the feedstock, pretreatment, and plant size

(A) Historical market prices of PET flakes.

(B) MSP of rTPA as a function of feedstock cost.

(C) Sensitivity analyses demonstrating variations in the pretreatment process section that exhibit the highest impact on rTPA selling price.

Abbreviations and symbols used— Φ_{PET} : fraction of PET (by weight in the feedstock, base case value = 0.95), MTPD, metric tons per day (base case value = 150 MTPD); NMP, no mechanical pretreatment. Numerical data in this figure are reported in Tables S11 and S12.

(MRFs),^{51,52} which, in turn, will affect the quality and price of reclaimed PET. Market reports indicate that the average price of mixed, baled PET in the US varies from \$0.14–0.48/kg, translating to clean PET flakes available at \$0.55–0.90/kg (Figure 3A).^{40,41} Due to the variability in cost, sensitivities of PET prices ranging from \$(−0.11) to \$1.10/kg are modeled (equivalent to −5 cents to 50 cents per pound of PET), where negative feedstock costs indicate a scenario where a landfill tipping fee is potentially avoided.^{40,53,54} As observed, the PET feedstock cost drives the greatest variability in selling prices, which range from \$0.71/kg to \$2.63/kg as modeled and exhibit a linear relationship with MSP (Figure 3B). Additionally, to accommodate the variability in relative PET content, PET fraction sensitivities of $\Phi = 0.99$ (e.g., clean mechanically recyclable grade) and $\Phi = 0.91$ (e.g., post-consumer curb side pickup grade but enriched in PET) are assessed.^{40,51,52} The relative PET content has minimal effect on MSP (\$0.17/kg).

Additional sensitivity cases explored in this case study include varying the plant size and modifying the pretreatment configuration (Figure 3C). The latter case considers an alternate design scenario where no mechanical pretreatment (NMP) is required, relying on the assumption that enzymes capable of activity on both crystalline and amorphous domains of PET are available, thereby rendering the pretreatment steps of extrusion, amorphization, and micronization unnecessary. By avoiding the mechanical pretreatment (NMP case) and achieving the same rate of depolymerization, the rTPA MSP can be lowered to \$1.69/kg.

Case study II: Enzymatic PET depolymerization

Next, we considered key variables in the enzymatic depolymerization section. Previous work from several research groups indicates that cost of enzyme production can range widely from \$25–\$110/kg depending on enzyme type, expression strategy, titers, extraction methods, and production scale.^{35,55,56} This is higher than the cost of fungal cellulases estimated in previous studies on biochemical conversion of lignocellulosic biomass, which are ~\$5/kg.^{57–59} For the base case model, enzyme purchase cost is set as \$15/kg and is varied in the sensitivity analysis (Figure 4A).^{60–63}

Aside from enzyme production, additional sensitivity parameters explored include enzyme loading and bioreactor residence time (τ). The base case design considers

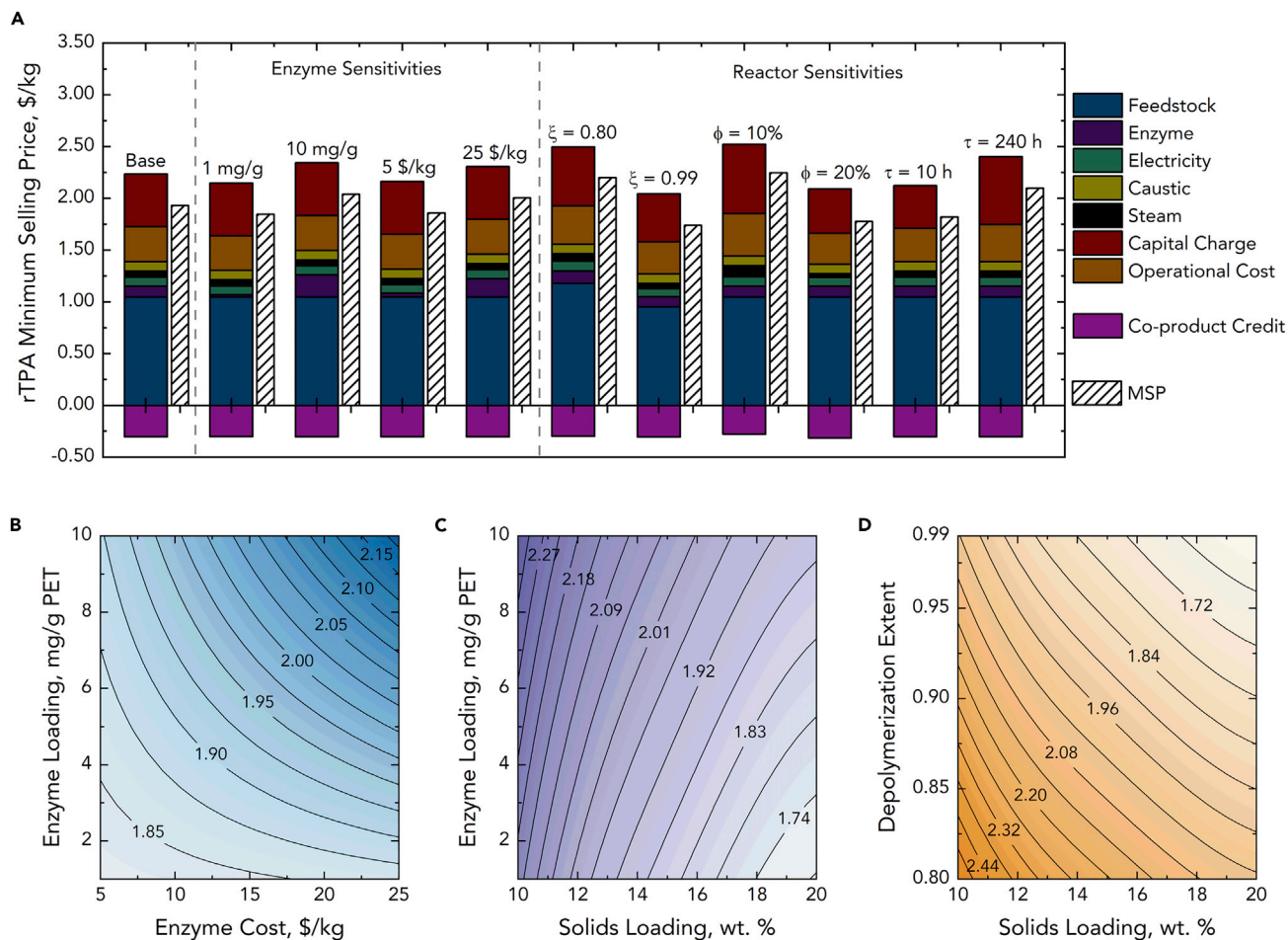


Figure 4. TEA sensitivity results for process parameters associated with the enzymatic depolymerization step

(A) Cost breakdown of the rTPA MSP in the base case process design and as a function of process variables including enzyme loading (mg/g PET feedstock, base case value = 5), enzyme price (\$/kg, base case value = 15) as well as sensitivities related to the reactor configuration, including extent of conversion (ξ base case value = 0.9), solids loading, wt % (ϕ base case value = 0.15), and residence time in hours (τ base case value = 96 h).

(B) Multivariate sensitivity analyses demonstrating the combination of enzyme cost and enzyme loading in which a decrease in both parameters exhibits a non-linear decrease in the selling price of rTPA.

(C) Multivariate sensitivity analyses demonstrating the combination of solids loading and enzyme loading, which affects the selling price of rTPA. Higher solids loading and lower enzyme loading results in reduction of the rTPA MSP.

(D) Multivariate sensitivity analyses demonstrating the combination of solids loading and extent of conversion in which lowering both parameters results in a decrease of TPA MSP. The contour lines serve as references to interpolate the MSP of rTPA (\$/kg). Numerical data in this figure are reported in Tables S15–S18.

these variables at an intermediate value of 5 mg enzyme/g of PET input and 96 h, respectively. Products of PET hydrolysis are recovered in this process scheme upon reaching a 90% PET degradation extent (the reaction scheme is shown in Figure S1).³⁵ Additionally, the generalized PET hydrolase modeled is assumed to have maximal degradation activity at 60°C and pH 8. PET hydrolases have been reported to function over a range of temperatures and pH values,⁶⁴ as well as a range of enzyme loading values; therefore, these values were also explored as sensitivity parameters. Temperature and pH had a negligible impact on MSP in the ranges explored—data provided in Table S13. The two factors with largest impact on MSP include solids loading (ϕ) for which a change from 10% to 20% results in a \$0.47/kg decrease in MSP between the two cases, and the extent of conversion (ξ) for which a change from 0.80 to 0.99 results in a \$0.46/kg decrease in MSP between the two limits.

In several cases, single-point sensitivity analyses are not sufficient to fully reveal process modeling insights, namely, when process variables are strongly coupled. Thus, several single-point sensitivity analyses were complemented with multivariate sensitivity analysis to understand the interaction of process variables and reveal examples of strongly non-linear relationships that affect the overall rTPA selling prices. Examples of significantly correlated variables studied here include enzyme loading and enzyme cost (Figure 4B), solids loading and enzyme loading (Figure 4C), as well as solids loading and extent of depolymerization (Figure 4D). As an illustrative example, solids loading coupled with the extent of depolymerization can not only drive the MSP of rTPA as low as \$1.60/kg in the range examined at the highest loadings/extents but can also drive costs to >\$2.50/kg at the lowest loadings and extents. An additional multivariate sensitivity exploring enzyme loading and depolymerization is shown in Table S14.

Case study III: Product and co-product recovery

Lastly, we investigated the process variables in the downstream processing section. Increasing the recovery of EG to 65% or rTPA to 98% will lower the MSP to \$1.87/kg (reduction by \$0.05/kg) or \$1.83/kg (reduction by \$0.10/kg), respectively, whereas reducing the selling price of EG and/or SS will lead to an increase in the overall MSP (Figure 5A). Changing the market price of EG by approximately 30% in either direction of the base case value (\$0.96/kg⁵⁰) changes the selling price of rTPA by \$0.12/kg between the two bounding cases. Since EG recovery leads to a significant steam usage in distillation, a case where more EG selective membranes⁴⁹ (99% EG retention selectivity, while SS selectivity remains the same) are depolymerized is modeled, which could potentially reduce the capital and operating expenses to run the distillation columns. MSP in this case can be lowered to \$1.75/kg and would have industry-wide implications in other EG/water recovery scenarios (EG Selective membrane, Figure 5A).

The base case, reported in the previous case studies, assumes that both EG and SS are recovered. Therefore, sensitivity cases around downstream process design were explored where recovery of co-products was changed (Figures 5B and 5C). Two scenarios, one in which no EG is recovered (NEG) and one where neither co-product is recovered (NCP), were considered. In the first scenario (NEG), when EG is not recovered but SS is, the EG-containing solution from the SS crystallizer is sent to wastewater treatment and the co-product credit associated with EG recovery is lost. The rTPA MSP in this scenario (NEG) corresponds to \$2.08/kg as shown in Figure 5B. In the second scenario (NCP) where neither EG nor SS is recovered, the mother liquor from the TPA crystallizer is sent to wastewater treatment and the revenue opportunity from both co-product sales is discounted. As a result, the capital investment and utilities required for SS and EG recovery are omitted in this scenario. A similar impact on the rTPA MSP is observed in the scenario exploring no co-product recovery (NCP), resulting in an increased MSP of \$2.10/kg (Figure 5B). Details on the additional wastewater treatment, co-product credit losses, and the capital expense tradeoffs can be found in Table S19.

Summary of TEA results

Based on the process variables examined in the three case studies/sections earlier, the results of those sensitivity analyses from Figures 3, 4, and 5 were summarized to rank cost drivers on rTPA MSP and are presented in the tornado plot (Figure 6; Table S21).

Within the parameter ranges chosen, feedstock cost is the largest contributor to the rTPA MSP. The feedstock modeled in this study is clean PET that meets quality standards for mechanical recycling⁵² and drove the greatest variability in rTPA MSP as

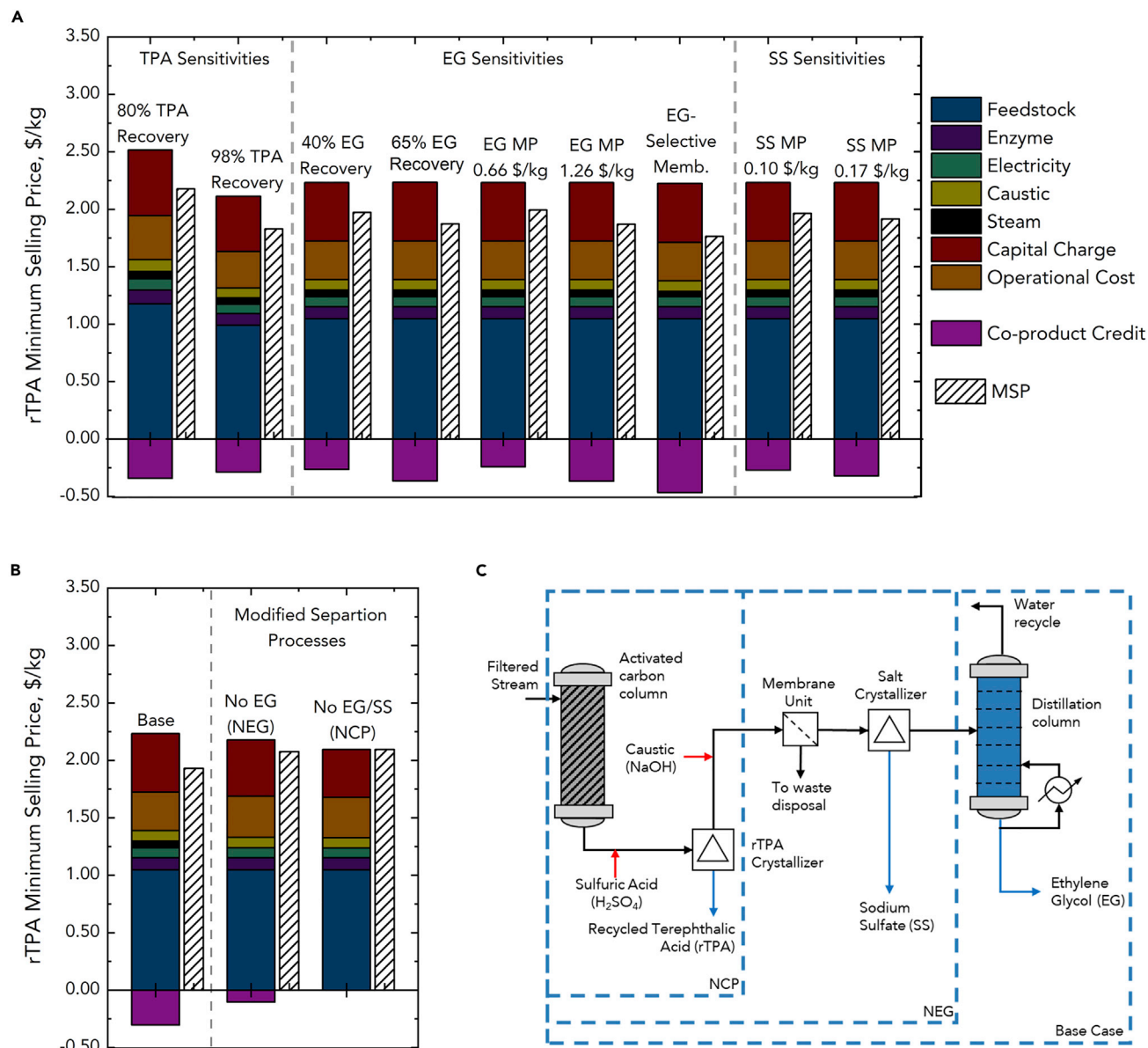


Figure 5. TEA sensitivity results for process parameters associated with product and co-product recovery

(A and B) (A) rTPA MSP for the base case (base case values: rTPA recovery = 90%; EG recovery = 50%; EG MP = \$0.96/kg; SS MP = \$0.15/kg) to indicate the effect of product and co-product recoveries as well as the co-product market prices (B) MSP as a result of different co-product recovery schemes without the co-product(s), illustrating that although operational expenses may decrease, MSP will increase because of the lack of a co-product credit. (C) Process flow diagram of the modified separation processes. Numerical data in this figure are reported in Table S20. Abbreviations used—MP, market price (for co-products, averaged over 5 years); NEG, no EG is recovered; NCP, no co-product is recovered.

also noted before (Figure 3A). Next, the effect of plant scale emerged important. A facility size of 50 MTPD would indicate a decentralized approach (with smaller collection radii) for building such enzymatic recycling facilities for PET, which increases the MSP from the base case by 26%, whereas 300 MTPD is being investigated to see the effect of economies of scale, which decreases the MSP by 5%.

Besides exogenous factors, such as feedstock price and plant size, the relatively high importance of depolymerization-related sensitivities such as solids loading and the extent of conversion stand out as the dominant factors affecting MSP, followed by

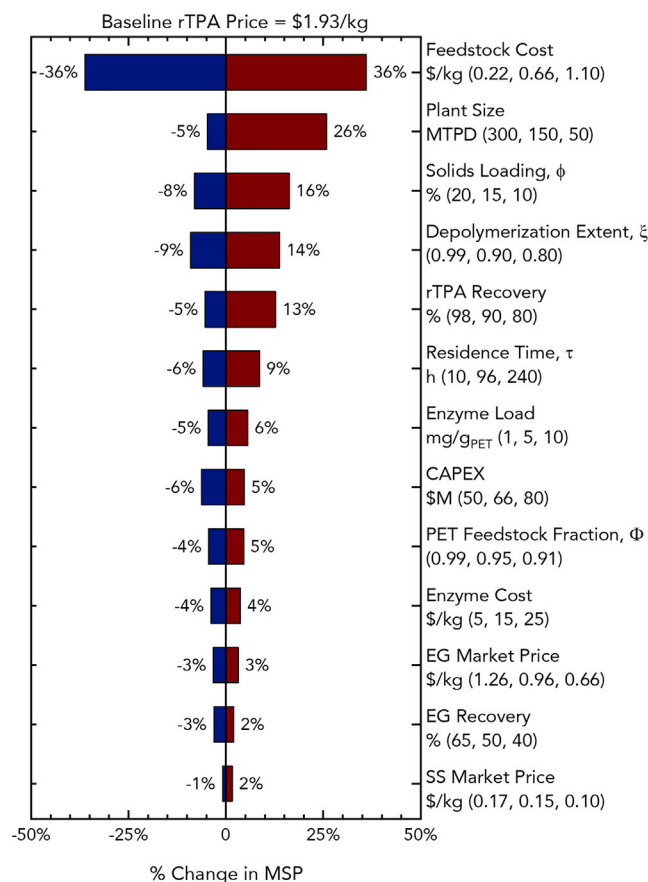


Figure 6. Tornado plot summarizing the effect of different process variables investigated on the rTPA MSP

Univariate analysis summarizing how process variables affect rTPA MSP across the three case studies of feedstock pretreatment, depolymerization, and product and co-product recovery. The rTPA MSP in the base case is \$1.93/kg. Factors not shown have a minimal effect in a univariate sensitivity analysis. Numerical data for this figure are reported in [Table S21](#).

overall TPA recovery. Residence time for batch hydrolysis and enzyme loading would be of particular interest to the research community, and these parameters could change the MSP by 5%–9% within the ranges examined. Variations in the total capital expense (+/– \$15M relative to the base case fixed capital investment) is also studied. Finally, the market price of co-products, varying over a 30% range, has a relatively minor impact on the overall MSP of rTPA.

Note that this tornado plot only includes key process variables in the base design and does not include the different process design (i.e., NMP, NEG, and NCP), but those design changes do have a significant impact on MSP, as noted. Additionally, the impact of variations in process design on the overall supply chain energy and GHG emissions, as well as broader socioeconomic effects, is discussed in the following sections.

Bottom-up analysis of supply chain energy and GHG emissions

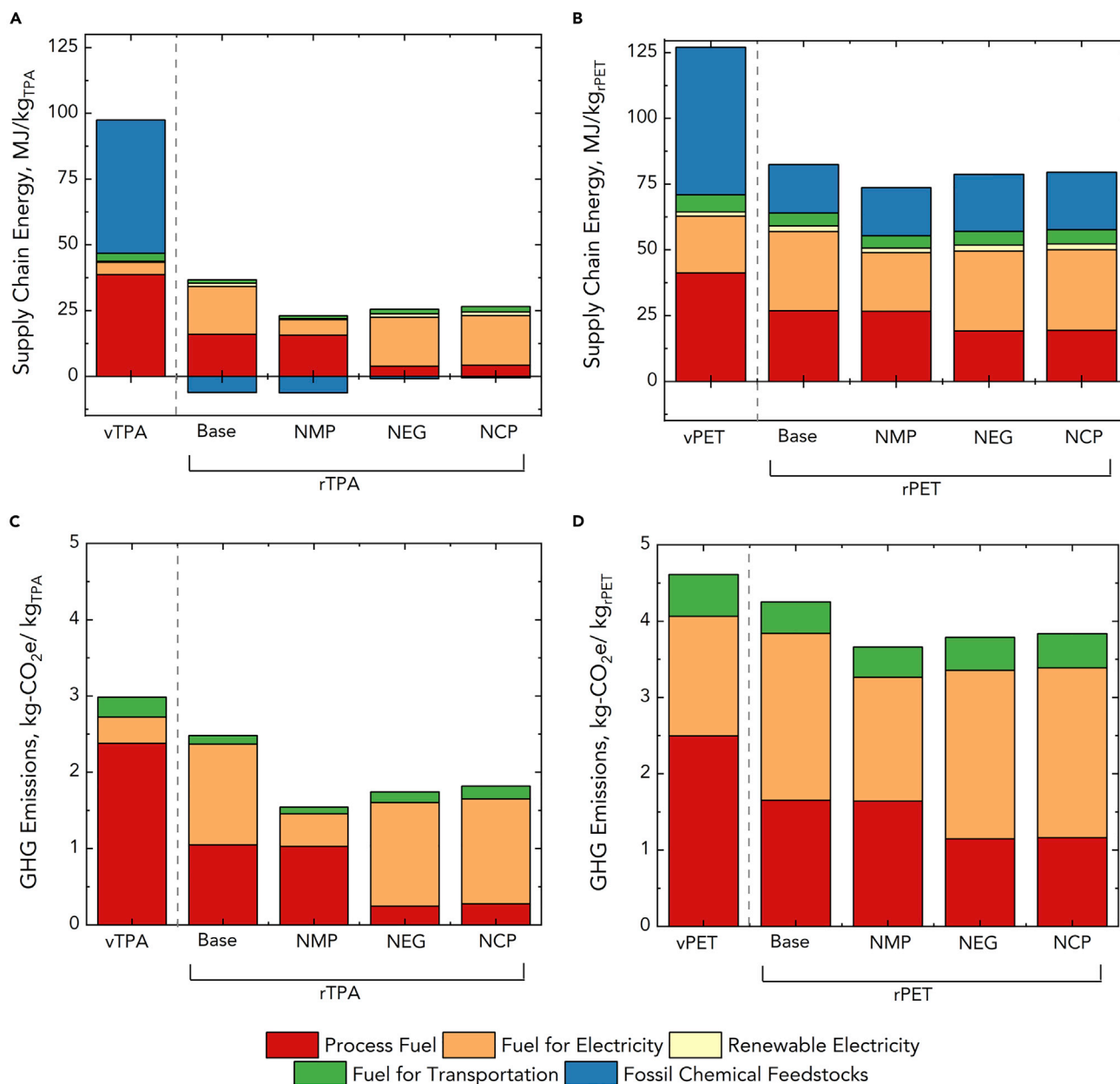
To quantify the energy and GHG emissions associated with the modeled supply chain, we employed MFI, a bottom-up, supply chain modeling tool.^{5,37,65} Specifically, MFI was used to compare the energy requirements and GHG emissions

associated with rTPA produced using enzymatic depolymerization with those of the conventional fossil feedstock-derived vTPA supply chain (see [Figure S5](#)). The results of the TEA modeling were integrated into the MFI database by connecting the process inputs from the Aspen Plus model to their corresponding representations in the MFI database of process inputs. The analysis conducted using MFI includes select sensitivities from the previously mentioned case studies.

When comparing rTPA and vTPA, it is necessary to consider the effect of the first life of the TPA (i.e., procurement, production, and polymerization into PET). To do so, we define the functional unit (our basis of comparison) to be the total number of PET “lifetimes” that can be obtained from repeatedly utilizing the enzymatic depolymerization process on the feedstock obtained from an initial quantity of 1 kg of fossil-derived PET. Given an overall yield from the enzymatic depolymerization process of 0.63 kg TPA/kg of depolymerized PET (current process design), and assuming that the requisite amount of rTPA required to manufacture new PET is approximately 0.87 kg TPA/kg PET (MFI process data), the recycled content of the rTPA-derived PET is approximately 72%. An infinite summation series can be constructed for multiple loops through the enzymatic recycling process, which converges to the “lifetime” amount of rTPA-derived PET that could be achieved from a given amount of fossil-derived waste PET feedstock. The total amount of PET is calculated to be 3.6 kg in the enzymatic depolymerization supply chain (see [supplemental experimental procedures](#), MFI methodology and [Figure S6](#) for the derivation), of which, 1 kg is fossil-derived and the remaining 2.6 kg is obtained from the enzymatic depolymerization process. The supply chain level impacts on this supply chain were compared with the analogous supply chain to produce 3.6 kg of PET from the conventional fossil-derived route. The results were then normalized to 1 kg of PET for simplicity.

Results from the base case and select MFI analyses are presented in [Figure 7](#) for rTPA and PET, which indicate that there is a significant estimated energy savings potential from enzymatic depolymerization-based supply chains. The conventional manufacturing supply chain for PET bottles requires ~ 127 MJ/kg, (as calculated by the MFI tool), whereas the enzymatic depolymerization supply chains require 74–82 MJ/kg, a reduction of 35%–42%. This reduction is primarily due to a sharp reduction in fossil feedstock energy requirements, from ~ 56 MJ fossil feedstock/kg PET for the conventional route to ~ 18 MJ fossil feedstock/kg PET for the enzymatic depolymerization route. In the latter route, fossil feedstocks arise from the production of other required supply chain inputs (e.g., sulfuric acid, caustic, etc.). Aside from supply chain energies, the base case and the NMP case are estimated to emit 8% and 21% lower GHG emissions per kg of PET, respectively, compared with the fossil-derived PET baseline, or 4.3 kg carbon dioxide equivalent (CO₂e)/kg PET and 3.7 kg CO₂e/kg PET, respectively. The reason for the discrepancy between percent energy reduction and percent GHG reduction is that fossil feedstock use, by definition, does not entail GHG emissions because the feedstock is not combusted, but converted into products (hence the blue bar does not appear in the bottom row of charts in [Figure 7](#)).

As also shown in [Figure 7A](#), when the system boundary is narrowed to exclude the polymerization step, monomer rTPA production from enzymatic depolymerization is estimated to consume 69%–83% less energy than conventional production of vTPA, mostly due to differences in feedstock energy requirements. In fact, the enzymatic depolymerization monomer production entails a negative feedstock energy contribution due to the offset from EG and SS co-production. GHG emissions impacts for monomer rTPA production exhibit a similar trend, with 17%–43% lower GHG emissions for enzymatic depolymerization compared with fossil-derived vTPA.



economic structure reflecting the respective technologies at an industry scale. Originally, BEIOM was developed to quantify the effects of an expanding US bio-economy, describing the potential benefits and unintended consequences of new bio-based technologies across several environmental and socioeconomic impact categories from a holistic perspective. Here, BEIOM is applied to compare the production of conventional vTPA with rTPA produced via enzymatic depolymerization. The inclusion of the rTPA production processes as a new sector in BEIOM followed the same procedure as previous work evaluating different bio-based processes.³⁸ Specifics on how each TPA pathway was integrated into BEIOM can be found in [supplemental experimental procedures](#) and [Figure S7](#), with detailed results illustrated in [Figures S8–S32](#).

The impacts of producing 1 kg of vTPA compared with 1 kg of rTPA include direct impacts (generated by the plant itself and its supply chain) and indirect impacts generated by related activities across all other sectors of the US economy ([Figure 8](#)). To quantify impacts on a per kg basis, the total impacts (direct and indirect) from either TPA production were divided by the total TPA output of the respective industry. Additional co-products (EG and SS) are accounted for and their impacts are allocated via substitution (on an economic basis). In the rTPA base case, EG and SS are both recovered. Two sensitivity cases are also modeled to evaluate scenarios where no EG is recovered (NEG), and where neither EG nor SS are recovered (NCP). We also model a scenario that recovers both co-products but excludes mechanical pretreatment (NMP).

We estimate that rTPA generates socioeconomic benefits for both added economic value and jobs, except in the NMP scenario where the exclusion of mechanical pretreatment reduces overall economic effects ([Figure 8A](#)). Further, the socioeconomic effects are more concentrated for rTPA in the conversion plant and its direct supply chain, whereas they are spread out more broadly across the economy for vTPA. Two thirds of the jobs from rTPA production are concentrated in the conversion process and the direct inputs for the process. Production of vTPA sustains more jobs further upstream in the production chain, where one third of the jobs are in the service sectors.

In the resource use metrics category ([Figure 8B](#)), rTPA shows a much higher water withdrawal than vTPA, except when mechanical pretreatment is excluded (NMP case). This is exclusively caused by water use accounted for in the US national electricity generation mix for 2017 and is a consequence of higher electricity consumption modeled to produce rTPA as compared with vTPA. It suggests that rTPA plants sourcing electricity with a low water footprint could alleviate this difference. Further, we find that rTPA reduces overall land occupation by at least 40% compared with vTPA. In both cases, the resource use impacts are mainly attributable to economic activities, related to, but beyond the rTPA plant and its supply chain, i.e., are indirect effects generated by the system within which the supply chains are operating in. Most land occupation effects are indirect (i.e., not attributable to the specific conversion facilities) and related to agriculture and the oil extraction sectors (land leases). For rTPA, 34% comes from forestry, 27% from grain farming, 12% from oil and gas extraction. For conventional TPA, oil and gas extraction effects increase to 25%, whereas forestry and grain farming effects are relatively similar to those from rTPA at 33% and 26%, respectively ([Figure S1](#)).

Across all (midpoint) life-cycle impact categories evaluated, rTPA shows an improvement in the domestic footprint by 10%–95% over vTPA ([Figure 8C](#)). vTPA impacts are mainly caused by the TPA production step across all metrics, whereas for rTPA, only the freshwater ecotoxicity is dominated by the production process. Instead, rTPA

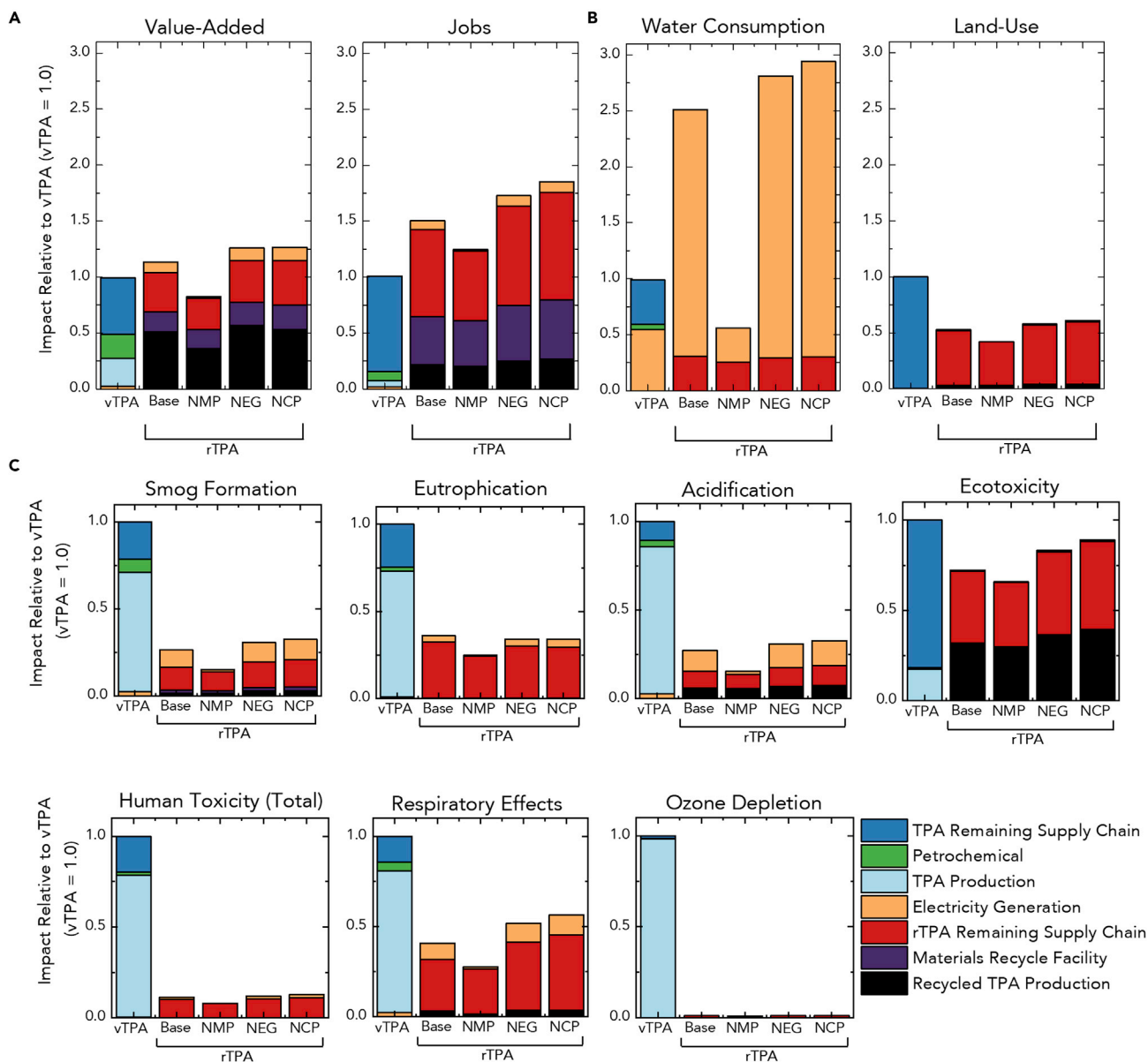


Figure 8. Socioeconomic and environmental impacts of producing 1 kg of TPA when accounting for the US economy-wide effects

(A–C) Impact from the production of 1 kg of TPA for each scenario presented for (A) socioeconomic, (B) resource use, and (C) environmental impact categories. Scenarios include the production of vTPA, rTPA (Base), rTPA with no mechanical pretreatment (NMP), rTPA with no EG recovery (NEG), and rTPA with no EG or SS recovery (NCP). Numerical data in this figure are reported in [Table S24](#).

impacts are largely caused by upstream processes. Electricity generation also contributes notably to smog formation, acidification, and respiratory effects in the rTPA cases.

Comparing the rTPA base case with the two co-product disposal sensitivity cases (NEG, NCP) in [Figure 8](#), we find that co-product recovery reduces the environmental effects across resource use and impact categories per kg of rTPA. Excluding the mechanical pretreatment step (NMP) reduces the environmental impacts of the base case (rTPA) by up to 65%; however, it also lowers the socioeconomic benefits by 10%–20%.

Capturing economy-wide effects expands the system boundary beyond the supply chain and generally increases the effects per metric (see Figure 8 “remaining supply chain” segments for vTPA and rTPA). Although the inclusion of indirect effects does not favor either one of the two products analyzed, its exclusion would alter results toward a further improvement of environmental benefits from rTPA while dramatically reducing the socioeconomic benefits attributable to vTPA.

DISCUSSION

In response to the pollution crisis caused by waste plastics, new recycling processes are needed for which requisite analyses will be critical to understanding the key cost drivers, supply chain impacts, barriers to scale-up, and market implementation. Here, we present a comprehensive analysis of enzyme-based PET recycling that includes rigorous process modeling, economic impacts of key process variables, supply chain energy, and GHG emissions impacts compared with fossil-based incumbent manufacturing, and examination of life cycle and socioeconomic impacts. These analyses demonstrate that enzyme-based PET recycling exhibits substantial promise, which can be improved with further process advancements, as detailed here.

Feedstock considerations

The current, global approach to PET recycling nearly universally employs mechanical recycling of post-consumer single-use PET bottles, and less than 20% of the eligible waste stream is processed in the US (less than 7% worldwide⁶⁷). Furthermore, mechanical recycling imposes stringent contamination tolerances,⁵² necessitating extensive preprocessing and cleaning steps, significantly impacting reclaimed PET flake prices.⁶⁸ Accordingly, plastic recycling technologies that are agnostic to the feedstock quality and expand the waste streams eligible for recycling will be effective in changing the recycling landscape.

The enzyme-based chemical recycling process presented here is one such prospective technology. Enzymatic recycling offers the advantage of high selectivity for the target PET substrate, thereby reducing the need for stringent contamination tolerances, opening up the pool of eligible waste feedstocks, and creating an opportunity for lower feedstock costs. Multiple feedstocks and conversion pathways should be considered for their economic and environmental impacts, and compared with mechanical recycling, which is already efficient but limited by the purity of the feedstock required. In the end, a combination of different technologies, ranging from mechanical recycling to more substrate selective chemical recycling, will likely need to be deployed to enable higher PET-recycling rates.

Size of the PET-recycling facility

Aside from feedstock cost, there are other engineering considerations that are key cost drivers in realizing an enzymatic recycling process for PET, including the facility size. The facility size will likely be dictated by local and regional collection rates and whether any incentives exist that encourage recycling participation (e.g., the US states with bottle deposit programs demonstrate higher collection volumes).³⁹ In this study, a plant with the capacity to process 150 MTPD was modeled. However, the operation of any recycling plant is dependent on securing a steady and sufficiently large feedstock supply. Considering that the largest MRFs in the US can process about 1,000 MTPD of post-consumer waste,⁶⁹ if the incoming waste stream is about 3.7% PET by weight⁷⁰ and a recovery of 91% PET can be obtained,⁷¹ only 33.7 Mt of PET could be secured from such a facility per day. This estimates that the largest MRFs in the country are unlikely to obtain more than 50 MTPD of PET that is suitable for mechanical recycling.

Although the advent of new technologies, including the enzymatic process presented here, may lead to an enhanced recycling capacity, this analysis highlights that it will still be necessary for any chemical recycling facilities to obtain PET-based feedstock from multiple MRFs, or to include additional sources of PET previously excluded from consideration for mechanical recycling, such as textiles, fibers, and layered packaging materials. It is important to note that the average distance for waste PET transport significantly varies throughout the US⁷² and in other parts of the world;^{73–77} therefore, additional factors may influence the economics if the plant size is increased. For example, in some regions, it might be necessary to establish centralized recycling facilities to increase the collection volumes of post-consumer PET⁷⁸ at the expense of greater transportation costs. Securing a consistent feedstock supply by analyzing statistical and geospatial distribution of plastic waste will be critical to de-risk the operation of any recycling facility.

Substrate considerations

Any requirement for size reduction of the feedstock and/or change in PET crystallinity will contribute to the economics, energy demands, and GHG emissions of the overall process. This is exemplified by the NMP case, which lowers rTPA MSP to \$1.70/kg (12% less than the baseline MSP), generates 38% lower GHG emissions, and requires 45% lower supply chain energies. Pretreatment that is akin to mechanical recycling has been proposed to enable greater enzymatic process efficiencies. Specifically, the recent study by Tournier et al. reports an engineered PET hydrolase enzyme capable of up to 85% product yield from post-consumer waste PET within 20 h of treatment,^{35,79,80} where the PET was pre-treated by extrusion, amorphization, and micronization to reduce the substrate crystallinity and size, respectively. Size reduction has also been proposed to enhance the extent of depolymerization by increasing the accessible surface area for enzyme action,⁸¹ however, systematic investigation is necessary to understanding the influence of these factors on enzyme performance. Additionally, the community will need to find an optimum size reduction that enables a high extent of depolymerization, desirable for increasing throughput, and beyond which the additional cost of size reduction may not be offset by incremental product yield.^{81–85}

Biocatalyst performance

Enzyme performance and optimization remains an open area of opportunity with important implications for the economics of an enzyme-based recycling process. Here, we highlight that solids loading, enzyme loading, and enzyme cost are key cost drivers; however, this is predicated on other assumptions in this model, the key among them being that the enzyme can achieve a high extent of depolymerization of the PET feedstock. To achieve a high extent of depolymerization, the global research community is investigating multiple parameters including the optimization of enzyme performance, specificity for substrates of different crystallinities, tolerance to inhibition by products and contaminants, and improved stability for enhanced catalytic lifetime.

The best-studied PET hydrolases to date are seemingly most active on the amorphous regions of the polymer.³⁴ Continued optimization and engineering of enzyme performance on PET substrates of different crystallinities will be critical, as the two largest applications of PET (bottles and fibers) exhibit high (30%–40%) crystallinity.⁸⁵ By leveraging enzyme design and exploring the use of thermophilic enzymes, improvements across multiple factors can be achieved. For instance, enzymes active at approximately 70°C may exploit the reduction in crystallinity as PET approaches its glass transition temperature. Enhanced thermostability may be engineered into

PET-degrading enzymes as shown by the stabilizing effect of glycosylation on leaf-compost cutinase (LCC),²⁸ or the replacement of a potential calcium-binding site in LCC with a disulfide bond³⁵; in each case, the thermal stabilization was accompanied by enhanced PET hydrolysis activity at an elevated temperature.

Enzyme design can also enable faster turnover, product selectivity, and inhibition resistance, all of which are ideal for mixed feedstock streams (e.g., textiles with dyes). Recently, accumulation of additives has been documented to inhibit cutinase activity,⁸¹ and therefore, methods to overcome inhibition, or remove contaminants,⁸⁶ could improve enzyme performance. In addition, given the inevitable acidification of the solution that occurs upon ester bond hydrolysis, any acid-tolerant PET-degrading enzymes that exhibit a broad pH optimum range would reduce the need to continually neutralize the depolymerization reaction, thus saving on caustic additive. Interestingly, acid-tolerant cutinases have been identified^{87–89} with an enzyme from the fungus *Thielavia terrestris* exhibiting esterase activity over the pH range 4–8 and detectable PET-degrading activity at pH 4.0 and 50°C.⁸⁷

Combining all of the properties mentioned earlier—thermostability, acid- and product-tolerance, and a high turnover of PET of varied crystallinities—represents a major challenge for future enzyme engineering efforts.

Enzyme production

Beyond enzyme function, the work presented here assumes that the enzyme is produced offsite, which leads to the MSP exhibiting a linear dependence with enzyme cost. Factors that drive enzyme production costs include the origin of the enzyme, the expression host, and the level of purification required for adequate activity. The price of generic hydrolase used in our base design is modeled after extracellular secretion from the host organism and concentration of the enzyme in the crude broth, without any elaborate purification. For intracellular protein production, purification requirements are key cost drivers.^{56,59,90–92} However, many industrial enzymes are secreted from the host therefore avoiding the processing steps associated with cell lysis.^{56,59,90} Stabilizing agents are also frequently used to ensure the longevity of the enzymes. However, consistent supply and compatibility of any stabilizers with enzyme function are important considerations in the development of an enzyme product.

The production of cellulase enzymes in filamentous fungi offers an analogous system for comparison and benchmarking, and this approach was used as the baseline for enzyme costs in the current work. In the case of cellulases, fungi such as *Trichoderma reesei* have been evolved and engineered over decades to secrete native and heterologous cellulases to extremely high levels (~protein concentrations on the order of 100 g/L).^{93,94} Thus, filamentous fungi offer an excellent starting point for future development of PET-active enzyme production. Alternative eukaryotic expression hosts may come to the forefront, for example, the methylotrophic yeast *Pichia pastoris*, which has been utilized for the recombinant expression of a variety of esterase enzymes.^{28,89,95–100} To date, laboratory-scale fermentations of *P. pastoris* have produced recombinant cutinases at yields up to 10.8 g/L.^{95,96,100}

Product and co-product recovery

Although pretreatment and enzyme optimization may influence the kinetics of PET hydrolysis, efficient product recovery will also have a major impact on the rTPA MSP, as this determines which products can be sold and at what purity. The process modeled here assumes that dyes, pigments, and adhesives are removed by the solid

filtration and activated carbon column.^{35,42–44} Spent enzymes are removed by ultrafiltration in the base case, which may not be a necessary step if there is sufficient removal by the activated carbon column,¹⁰¹ thereby resulting in a lower MSP. Although this design is aligned with reported practices, alternate and emergent separation techniques for product recovery can be potentially explored. For example, TPA could be recovered by sublimation in a process akin to that developed by Eastman.¹⁰² The recovery of EG is contingent on the fact that all the added SS salt is recovered from the solution prior to sending it to distillation columns, which remains to be verified. As the recovery of EG is an energy-intensive process,^{103,104} alternative separation schemes, (e.g., liquid-liquid extraction, membrane-based separations, condensed phase chromatographic separations techniques, reactive distillation followed by hydrolysis, etc.) could also be explored, which may eventually reduce the MSP and process energy requirements.^{44,103,105–113}

Sustainability impacts

In terms of the environmental impact analysis of the supply chain modeling, it is clear that a reduction in feedstock energy (in the form of natural gas and crude oil) is a primary contributor to the estimated reduction in supply chain energy for the enzymatic depolymerization relative to fossil-derived routes to PET. However, feedstock energy alone does not offer an opportunity to reduce GHG emissions (since feedstocks are, by definition, not combusted). Process-based energy requirements (e.g., from steam utilization) are shown to be significantly reduced in the enzymatic depolymerization routes at the expense of increased electricity usage. GHG emissions associated with the supply chain's electricity requirements are highly dependent on the assumed grid mix of generation technologies. MFI supply chain models reflect current industrial practices within the US industry; for electricity specifically, MFI assumes a national grid mix as of 2016.¹¹⁴ Since the modeled enzymatic depolymerization supply chain has been shown to be relatively more electricity-intensive than conventional PET production, additional GHG emissions reductions could be realized with an underlying electricity grid mix having a higher penetration of lower- or non-GHG-emitting, renewable (e.g., solar and wind) generation sources.

Furthermore, analysis with BEIOM highlights that, within the rTPA plant design, the crystallization process might warrant a more in-depth assessment to reduce process emissions. In the present design, it shows the highest share of process emissions and resulting relative contributions to the impact categories assessed (Figure S30). Sulfuric acid emissions are driving ecotoxicity and acidification impacts; EG (a regulated hazardous air pollutant) is driving human toxicity; both EG and sulfuric acid affect smog formation, along with volatile organic compounds from equipment leaks.

Social and environmental equity

The economy-wide comparison of vTPA and rTPA shows that the environmental and socioeconomic effects of the two processes are distributed unequally across their supply chain tiers (see also Figure S10). Environmental impacts from vTPA largely result from the production process itself, whereas its socioeconomic benefits mainly occur across the broader economy and are not necessarily regional. The distribution of effects from rTPA are reversed with socioeconomic benefits largely occurring at the facility itself and its direct suppliers, whereas most environmental impacts result from indirect activities further away from the rTPA supply chain. To account for and detail these social and environmental equity considerations, future analysis should further specify effects in regional contexts and recommend process alterations, if possible, to achieve an appropriate balance.

Beyond conventional substrates for recycling

Given the considerations presented, this work provides targets for process development toward realizing a more comprehensive recycling strategy than is available today. Leveraging the selectivity of biological depolymerization offers the opportunity to process mixed waste plastics and expand the eligible range of feedstocks. This concept can be extended to an integrated depolymerization refinery where the action of a cocktail of enzymes could break down the mixed plastic waste stream in a one-pot or tandem fashion. Changing feedstock, especially to materials that are not recycled today, would also allow for expanded plant sizes to offer the benefit of economies of scale for processing varied plastic types at higher volumes, particularly since PET bottles comprise only 30% of all PET produced globally. Other forms of PET waste, including discarded fabrics, textiles, and waste carpets (polyester fibers) comprised 44 MMT (or 54%) of global PET demand in 2019⁶ also present an opportunity for the application of enzyme-based recycling.

Importantly, the recycling approach described here will likely mirror the enzyme-based processing of other polymers, especially those that contain linkages that mirror natural polymers (e.g., nylons, polyurethanes, polycarbonates).^{115,116} Although each polymer will exhibit its own unique challenges, they may have similar characteristics that increase their ease of recycling. As an illustrative example, polyurethanes frequently feature crosslinking, which may limit access to enzyme activity or slow reaction rates; however, polyurethanes may also have a lower glass transition temperature and present a higher surface area, features that may accelerate reaction kinetics.¹⁹ The enzymatic recycling process model and subsequent analyses described here can therefore provide a foundation for evaluating other new enzymatic technologies, as well as broad guidance for the developing field.

Conclusions

Here, we describe the process design of an enzyme-catalyzed PET-recycling process and discuss the key factors impacting the process economics, supply chain energy, GHG emissions, socioeconomic impacts, and job creation potential for the enzyme-based recycling strategy as compared with the fossil-derived production currently employed. The TEA results estimate the potential for rTPA production at \$1.93/kg, and the study outlines certain scenarios to further reduce costs. In terms of pretreatment, feedstock prices and mechanical preprocessing are the largest contributing steps to cost and energy requirements. Meanwhile, in the depolymerization process, the extent of PET breakdown, solids loading, enzyme price, and enzyme loading are all key cost drivers. Importantly, the yields of recovered TPA and co-products (i.e., SS and EG) dictate the overall throughput of the plant and significantly impacts the economics. Supply chain analysis shows that PET recycling via the enzymatic route has lower supply chain energy requirement and lower supply chain GHG emissions compared to vTPA. An economy-wide assessment shows the potential socioeconomic (and largely regional) benefits of adding a plastics recycling sector and details environmental impacts per process and supply chain steps to highlight potential improvement areas for reducing unintended environmental consequences. There are multiple technologies in development as an alternative to the current mechanical PET-recycling strategies (e.g., chemo-catalytic, pyrolysis, etc.) of which enzymatic recycling offers the benefit of providing substrate specificity for complex mixed feedstock streams. Although the framework provided here is focused on PET reclaimed from an MRF, the insights presented here apply more broadly to polymeric systems that are susceptible to enzymatic depolymerization.

EXPERIMENTAL PROCEDURES

Resource availability

Lead contact

Further information and requests for resources and materials should be directed to and will be fulfilled by the lead contact, Gregg T. Beckham (gregg.beckham@nrel.gov).

Materials availability

This study did not generate new unique materials.

Data and code availability

The datasets in this article are provided in full in the supplemental information. The Aspen Plus models can be provided upon request and can be replicated by the inputs shown in the detailed PFD in the supplemental information.

The MFI tool is freely available to interested users on the NREL website. Accounts can be created there to use the tool. There are restrictions to the availability of the MFI code and database due to the proprietary nature of several process inventory datasets used by the tool.

Methods are described throughout the main text and in detail in the supplemental information where appropriate. In general, Aspen Plus models were constructed for all process and TEA analysis. MFI and BEIOM were used to quantify various supply chain and economy-wide effects.

SUPPLEMENTAL INFORMATION

Supplemental information can be found online at <https://doi.org/10.1016/j.joule.2021.06.015>.

ACKNOWLEDGMENTS

This work was authored in part by Alliance for Sustainable Energy, LLC, the manager and operator of the National Renewable Energy Laboratory for the U.S. Department of Energy (DOE) under contract no. DE-AC36-08GO28308. Funding was provided by the US Department of Energy, Office of Energy Efficiency and Renewable Energy, Advanced Manufacturing Office (AMO) and Bioenergy Technologies Office (BETO). This work was performed as part of the Bio-Optimized Technologies to keep Thermoplastics out of Landfills and the Environment (BOTTLE) Consortium and was supported by AMO and BETO under contract no. DE-AC36-08GO28308 with the National Renewable Energy Laboratory (NREL), operated by Alliance for Sustainable Energy, LLC. The BOTTLE Consortium includes members from the University of Portsmouth, funded under contract no. DE-AC36-08GO28308 with NREL and additionally supported by Research England (E3 scheme). The views expressed in the article do not necessarily represent the views of the DOE or the U.S. Government. The U.S. Government retains and the publisher, by accepting the article for publication, acknowledges that the U.S. Government retains a nonexclusive, paid-up, irrevocable, worldwide license to publish or reproduce the published form of this work, or allow others to do so, for U.S. Government purposes. We thank our colleagues in the BOTTLE Consortium for helpful discussions and Ryan Davis and Emily Newes for a critical reading of the paper.

AUTHOR CONTRIBUTIONS

A.S. and J.S.D. developed the process and economic models. N.A.R., A.R.P., J.E.M., E.E., and G.T.B. contributed to the process design and analysis. S.R.N. and A.C.C. conducted the supply chain modeling. A.F.T.A., P.L., Y.Z., A.B., and G.A. conducted

the economy-wide modeling. A.S., N.A.R., S.R.N., E.E., P.L., and G.T.B. wrote the manuscript with contributions from all authors.

DECLARATION OF INTERESTS

G.T.B., N.A.R., E.E., A.R.P., J.E.M., and G.T.B. have submitted patent applications on enzymes for PET recycling. N.A.R. and G.T.B. have submitted patent applications on upcycled materials from PET.

INCLUSION AND DIVERSITY

One or more of the authors of this paper self-identifies as an underrepresented ethnic minority in science. One or more of the authors of this paper self-identifies as a member of the LGBTQ+ community. While citing references scientifically relevant for this work, we also actively worked to promote gender balance in our reference list.

Received: March 16, 2021

Revised: May 16, 2021

Accepted: June 16, 2021

Published: July 15, 2021

REFERENCES

- Geyer, R., Jambeck, J.R., and Law, K.L. (2017). Production, use, and fate of all plastics ever made. *Sci. Adv.* 3, e1700782.
- Jambeck, J.R., Geyer, R., Wilcox, C., Siegler, T.R., Perryman, M., Andrady, A., Narayan, R., and Law, K.L. (2015). Marine pollution. Plastic waste inputs from land into the ocean. *Science* 347, 768–771.
- Law, K.L., Starr, N., Siegler, T.R., Jambeck, J.R., Mallos, N.J., and Leonard, G.H. (2020). The United States' contribution of plastic waste to land and ocean. *Sci. Adv.* 6, eabd0288.
- Rahimi, A., and Garcia, J.M. (2017). Chemical recycling of waste plastics for new materials production. *Nat. Rev. Chem.* 1, 0046.
- Nicholson, S.R., Rorrer, N.A., Carpenter, A.C., and Beckham, G.T. (2021). Manufacturing energy and greenhouse gas emissions associated with plastics consumption. *Joule* 5, 673–686.
- Bescond, A.-S., and Pujari, A. (2020). PET polymer. In *Chemical Economics Handbook (IHS Markit)*, p. 32. <https://ihsmarkit.com/products/chemical-economics-handbooks.html>.
- Nayak, A., Pujari, A., and Sharma, S. (2020). Polyethylene terephthalate (PET) solid-state resins. In *Chemical Economics Handbook (IHS Markit)*, p. 10. <https://ihsmarkit.com/products/polyethylene-terephthalate-resins-chemical-economics-handbook.html>.
- Ormonde, E., Loechner, U., Yoneyama, M., and Zhu, X. (2019). Plastics recycling. *Chemical Economics Handbook (IHS Markit)*, p. 56. <https://ihsmarkit.com/products/plastics-recycling-chemical-economics-handbook.html>.
- Sinha, V., Patel, M.R., and Patel, J.V. (2010). PET waste management by chemical recycling: a review. *J. Polym. Environ.* 18, 8–25.
- Paszun, D., and Spychaj, T. (1997). Chemical recycling of poly (ethylene terephthalate). *Ind. Eng. Chem. Res.* 36, 1373–1383.
- Pollard, M., Beisson, F., Li, Y., and Ohlrogge, J.B. (2008). Building lipid barriers: biosynthesis of cutin and suberin. *Trends Plant Sci.* 13, 236–246.
- Ralph, J. (2010). Hydroxycinnamates in lignification. *Phytochem. Rev.* 9, 65–83.
- Scheller, H.V., and Ulvskov, P. (2010). Hemicelluloses. *Annu. Rev. Plant Biol.* 61, 263–289.
- Ronkvist, Å.M., Xie, W., Lu, W., and Gross, R.A. (2009). Cutinase-catalyzed hydrolysis of poly (ethylene terephthalate). *Macromolecules* 42, 5128–5138.
- Loredo-Treviño, A., Gutiérrez-Sánchez, G., Rodríguez-Herrera, R., and Aguilar, C.N. (2012). Microbial enzymes involved in polyurethane biodegradation: a review. *J. Polym. Environ.* 20, 258–265.
- Sulaiman, S., Yamato, S., Kanaya, E., Kim, J.J., Koga, Y., Takano, K., and Kanaya, S. (2012). Isolation of a novel cutinase homolog with polyethylene terephthalate-degrading activity from leaf-branch compost by using a metagenomic approach. *Appl. Environ. Microbiol.* 78, 1556–1562.
- Roth, C., Wei, R., Oeser, T., Then, J., Föllner, C., Zimmermann, W., and Sträter, N. (2014). Structural and functional studies on a thermostable polyethylene terephthalate degrading hydrolase from *Thermobifida fusca*. *Appl. Microbiol. Biotechnol.* 98, 7815–7823.
- Yoshida, S., Hiraga, K., Takehana, T., Taniguchi, I., Yamaji, H., Maeda, Y., Toyohara, K., Miyamoto, K., Kimura, Y., and Oda, K. (2016). A bacterium that degrades and assimilates poly (ethylene terephthalate). *Science* 351, 1196–1199.
- Magnin, A., Pollet, E., Phalip, V., and Avérous, L. (2020). Evaluation of biological degradation of polyurethanes. *Biotechnol. Adv.* 39, 107457.
- Han, X., Liu, W., Huang, J.W., Ma, J., Zheng, Y., Ko, T.P., Xu, L., Cheng, Y.S., Chen, C.C., and Guo, R.T. (2017). Structural insight into catalytic mechanism of PET hydrolase. *Nat. Commun.* 8, 2106.
- Wei, R., and Zimmermann, W. (2017). Biocatalysis as a green route for recycling the recalcitrant plastic polyethylene terephthalate. *Microb. Biotechnol.* 10, 1302–1307.
- Wei, R., and Zimmermann, W. (2017). Microbial enzymes for the recycling of recalcitrant petroleum-based plastics: how far are we? *Microb. Biotechnol.* 10, 1308–1322.
- Austin, H.P., Allen, M.D., Donohoe, B.S., Rorrer, N.A., Kearns, F.L., Silveira, R.L., Pollard, B.C., Dominick, G., Duman, R., El Omari, K., et al. (2018). Characterization and engineering of a plastic-degrading aromatic polyesterase. *Proc. Natl. Acad. Sci. USA* 115, E4350–E4357.
- Danso, D., Schmeisser, C., Chow, J., Zimmermann, W., Wei, R., Leggewie, C., Li, X., Hazen, T., and Streit, W.R. (2018). New insights into the function and global distribution of polyethylene terephthalate (PET)-degrading bacteria and enzymes in marine and terrestrial metagenomes. *Appl. Environ. Microbiol.* 84, 02773–02717.
- Fecker, T., Galaz-Davison, P., Engelberger, F., Narui, Y., Sotomayor, M., Parra, L.P., and Ramírez-Sarmiento, C.A. (2018). Active site flexibility as a hallmark for efficient PET degradation by *I. sakaiensis* PETase. *Biophys. J.* 114, 1302–1312.

26. Joo, S., Cho, I.J., Seo, H., Son, H.F., Sagong, H.Y., Shin, T.J., Choi, S.Y., Lee, S.Y., and Kim, K.J. (2018). Structural insight into molecular mechanism of poly (ethylene terephthalate) degradation. *Nat. Commun.* **9**, 382.
27. Nikolaivits, E., Kanelli, M., Dimarogona, M., and Topakas, E. (2018). A middle-aged enzyme still in its prime: recent advances in the field of cutinases. *Catalysts* **8**, 612.
28. Shirke, A.N., White, C., Englaender, J.A., Zwarycz, A., Butterfoss, G.L., Linhardt, R.J., and Gross, R.A. (2018). Stabilizing leaf and branch compost cutinase (LCC) with glycosylation: mechanism and effect on PET hydrolysis. *Biochemistry* **57**, 1190–1200.
29. Su, A., Shirke, A., Baik, J., Zou, Y., and Gross, R. (2018). Immobilized cutinases: preparation, solvent tolerance and thermal stability. *Enzyme Microb. Technol.* **116**, 33–40.
30. Danso, D., Chow, J., and Streit, W.R. (2019). Plastics: environmental and biotechnological perspectives on microbial degradation. *Appl. Environ. Microbiol.* **85**, 01019–010195.
31. Furukawa, M., Kawakami, N., Tomizawa, A., and Miyamoto, K. (2019). Efficient degradation of poly (ethylene terephthalate) with *Thermobifida fusca* cutinase exhibiting improved catalytic activity generated using mutagenesis and additive-based approaches. *Sci. Rep.* **9**, 16038.
32. Palm, G.J., Reisky, L., Böttcher, D., Müller, H., Michels, E.A.P., Walczak, M.C., Berndt, L., Weiss, M.S., Bornscheuer, U.T., and Weber, G. (2019). Structure of the plastic-degrading *Ideonella sakaiensis* MHETase bound to a substrate. *Nat. Commun.* **10**, 1717.
33. Son, H.F., Cho, I.J., Joo, S., Seo, H., Sagong, H.-Y., Choi, S.Y., Lee, S.Y., and Kim, K.-J. (2019). Rational protein engineering of thermo-stable PETase from *Ideonella sakaiensis* for highly efficient PET degradation. *ACS Catal.* **9**, 3519–3526.
34. Taniguchi, I., Yoshida, S., Hiraga, K., Miyamoto, K., Kimura, Y., and Oda, K. (2019). Biodegradation of PET: current status and application aspects. *ACS Catal.* **9**, 4089–4105.
35. Tournier, V., Topham, C.M., Gilles, A., David, B., Folgoas, C., Moya-Leclair, E., Kamionka, E., Desrousseaux, M.L., Texier, H., Gavalda, S., et al. (2020). An engineered PET depolymerase to break down and recycle plastic bottles. *Nature* **580**, 216–219.
36. Knott, B.C., Erickson, E., Allen, M.D., Gado, J.E., Graham, R., Kearns, F.L., Pardo, I., Topuzlu, E., Anderson, J.J., Austin, H.P., et al. (2020). Characterization and engineering of a two-enzyme system for plastics depolymerization. *Proc. Natl. Acad. Sci. USA* **117**, 25476–25485.
37. Hanes, R.J., and Carpenter, A. (2017). Evaluating opportunities to improve material and energy impacts in commodity supply chains. *Environ. Syst. Decis.* **37**, 6–12.
38. Lamers, P., Avelino, A.F.T., Zhang, Y., Tan, E.C.D., Young, B., Vendries, J., and Chum, H. (2021). Potential socioeconomic and environmental effects of an expanding U.S. bioeconomy: an assessment of near-commercial cellulosic biofuel pathways. *Environ. Sci. Technol.* **55**, 5496–5505.
39. NAPCOR (2018). 2017 PET recycling report (National Association for PET Container Resources (NAPCOR)). <https://napcor.com/reports-resources/>.
40. Recycling Markets (2021). Secondary materials pricing. <https://www.recyclingmarkets.net/>.
41. Closed Loop Partners (2017). Cleaning the rPET Stream: How We Scale Post-Consumer Recycled PET in the US (Closed Loop Partners). <https://www.mitchellwilliamslaw.com/webfiles/2%20Cleaning%20your%20rPET%20Stream%20.pdf>.
42. Chateau, M. (2020). Method for producing terephthalic acid on an industrial scale (World Patent No. WO 2020/094661 A1) (World Intellectual Property Organization (WIPO)).
43. Karp, E.M., Cywar, R.M., Manker, L.P., Saboe, P.O., Nimlos, C.T., Salvachúa, D., Wang, X., Black, B.A., Reed, M.L., Michener, W.E., et al. (2018). Post-fermentation recovery of biobased carboxylic acids. *ACS Sustainable Chem. Eng.* **6**, 15273–15283.
44. Brown, G.E., Jr., and O'Brien, R.C. (1976). Method for recovering terephthalic acid and ethylene glycol from polyester materials (U.S. Patent No. US 3952053) (U.S. Patent and Trademark Office).
45. Fard, M.H., and Vakili, M.H. (2010). Chemical recycling of poly ethylene terephthalate wastes. *World Applied Sciences Journal* **8**, 839–846.
46. Lamparter, R.A., Barna, B.A., and Johnsrud, D.R. (1985). Process for recovering terephthalic acid from waste polyethylene terephthalate (U.S. Patent No. US 4542239) (U.S. Patent and Trademark Office).
47. Jehle, W., Staneff, T., Wagner, B., and Steinwandel, J. (1995). Separation of glycol and water from coolant liquids by evaporation, reverse osmosis and pervaporation. *J. Membr. Sci.* **102**, 9–19.
48. Li, W., Van der Bruggen, B., and Luis, P. (2014). Integration of reverse osmosis and membrane crystallization for sodium sulphate recovery. *Chem. Eng. Technol.* **85**, 57–68.
49. Biancari, A., Palma, L.D., Ferrantelli, P., and Merli, C. (2003). Ethylene glycol recovery from dilute aqueous solution. *Environ. Eng. Sci.* **20**, 103–110.
50. Chang, R.J., and Lacson, J. (2020). Process Economics Tool - PEP Yearbook (IHS Markit).
51. Eriksen, M.K., Damgaard, A., Boldrin, A., and Astrup, T.F. (2019). Quality assessment and circularity potential of recovery systems for household plastic waste. *J. Ind. Ecol.* **23**, 156–168.
52. The Association of Plastics Recyclers – APR. (2021). PET Resin specifications. <https://plasticsrecycling.org/markets/model-bale-specs/pet-resin-specifications>.
53. Moore, P., and Staub, C. (2020). Slipping through the Cracks. *Plastics Recycling Update*. <https://resource-recycling.com/plastics/2020/05/19/slipping-through-the-cracks/>.
54. Enviros consulting. (2009). MRF quality assessment study. Project Code: MRF011. <https://docplayer.net/20953314-Mrf-quality-assessment-study.html>.
55. Ferreira, R.D.G., Azzoni, A.R., and Freitas, S. (2018). Techno-economic analysis of the industrial production of a low-cost enzyme using *E. coli*: the case of recombinant beta-glucosidase. *Biotechnol. Biofuels* **11**, 81.
56. Mcvey, T.F. (2002). Industrial enzymes process economics program report - 139A (IHS Markit, SRI Consulting). <https://ihsmarkit.com/products/chemical-technology-pep-industrial-enzymes-2002.html>.
57. Davis, R.E., Grundl, N.J., Tao, L., Bidy, M.J., Tan, E.C., Beckham, G.T., Humbird, D., Thompson, D.N., and Roni, M.S. (2018). Process design and economics for the conversion of lignocellulosic biomass to hydrocarbon fuels and coproducts: 2018 biochemical design case update; biochemical deconstruction and conversion of biomass to fuels and products via integrated biorefinery pathways (National Renewable Energy Laboratory (NREL)), NREL/TP-5100-71949. <https://www.nrel.gov/docs/fy19osti/71949.pdf>.
58. Humbird, D., Davis, R., Tao, L., Kinchin, C., Hsu, D., Aden, A., Schoen, P., Lukas, J., Olthof, B., and Worley, M. (2011). Process design and economics for biochemical conversion of lignocellulosic biomass to ethanol: dilute-acid pretreatment and enzymatic hydrolysis of corn stover (National Renewable Energy Laboratory(NREL)), Technical Report NREL/TP-5100-47764. <https://www.nrel.gov/docs/fy11osti/47764.pdf>.
59. Klein-Marcuschamer, D., Oleskowicz-Popiel, P., Simmons, B.A., and Blanch, H.W. (2012). The challenge of enzyme cost in the production of lignocellulosic biofuels. *Biotechnol. Bioeng.* **109**, 1083–1087.
60. Bidy, M.J., Davis, R., Humbird, D., Tao, L., Dowe, N., Guarnieri, M.T., Linger, J.G., Karp, E.M., Salvachúa, D., Vardon, D.R., and Beckham, G.T. (2016). The techno-economic basis for coproduct manufacturing to enable hydrocarbon fuel production from lignocellulosic biomass. *ACS Sustainable Chem. Eng.* **4**, 3196–3211.
61. Gregg, D.J., Boussaid, A., and Saddler, J.N. (1998). Techno-economic evaluations of a generic wood-to-ethanol process: effect of increased cellulose yields and enzyme recycle. *Bioresour. Technol.* **63**, 7–12.
62. Sassner, P., and Zacchi, G. (2008). Integration options for high energy efficiency and improved economics in a wood-to-ethanol process. *Biotechnol. Biofuels* **1**, 4.
63. Wingren, A., Galbe, M., and Zacchi, G. (2003). Techno-economic evaluation of producing ethanol from softwood: comparison of SSF and SHF and identification of bottlenecks. *Biotechnol. Prog.* **19**, 1109–1117.
64. Kawai, F., Kawabata, T., and Oda, M. (2020). Current state and perspectives related to the polyethylene terephthalate hydrolases available for biorecycling. *ACS Sustainable Chem. Eng.* **8**, 8894–8908.

65. Rorrer, N.A., Nicholson, S., Carpenter, A., Bidy, M.J., Grundl, N.J., and Beckham, G.T. (2019). Combining reclaimed PET with bio-based monomers enables plastics upcycling. *Joule* 3, 1006–1027.
66. Lamers, P. Bio-based circular carbon economy environmentally-extended input-output Model (BEIOM). <https://bioenergymodels.nrel.gov/models/42/>.
67. World Economic Forum, Ellen MacArthur Foundation, and McKinsey & Company (2015). Project MainStream – a global collaboration to accelerate the transition towards the circular economy: status update. http://www3.weforum.org/docs/WEF_Project_Mainstream_Status_2015.pdf.
68. Awaja, F., and Pavel, D. (2005). Recycling of PET. *Eur. Polym. J.* 41, 1453–1477.
69. Powell, J. (2018). Sortation by the numbers. <https://resource-recycling.com/recycling/2018/10/01/sortation-by-the-numbers/>.
70. Combs, A.R. (2011). Life cycle analysis of recycling facilities in a carbon constrained world. <https://repository.lib.ncsu.edu/handle/1840.16/7808>.
71. Raymond, A.G. (2017). Modeling of material recovery facility performance with applications for life cycle assessment, PhD thesis (Massachusetts Institute of Technology).
72. Kuczynski, B., Geyer, R., and Bren, D. (2011). Life cycle assessment of polyethylene terephthalate (PET) beverage bottles consumed in the state of California (Department of Resources Recycling and Recovery). <https://www2.calrecycle.ca.gov/Publications/Details/1487>.
73. Merrill, H., Larsen, A.W., and Christensen, T.H. (2012). Assessing recycling versus incineration of key materials in municipal waste: the importance of efficient energy recovery and transport distances. *Waste Manag* 32, 1009–1018.
74. Chen, X., Xi, F., Geng, Y., and Fujita, T. (2011). The potential environmental gains from recycling waste plastics: simulation of transferring recycling and recovery technologies to Shenyang, China. *Waste Manag.* 31, 168–179.
75. Nakatani, J., Fujii, M., Moriguchi, Y., and Hirao, M. (2010). Life-cycle assessment of domestic and transboundary recycling of post-consumer PET bottles. *Int. J. Life Cycle Assess.* 15, 590–597.
76. Shen, L., Worrell, E., and Patel, M.K. (2010). Open-loop recycling: a LCA case study of PET bottle-to-fibre recycling. *Resour. Conserv. Recycl.* 55, 34–52.
77. Martin, E.J.P., Oliveira, D.S.B.L., Oliveira, L.S.B.L., and Bezerra, B.S. (2020). Dataset for life cycle assessment of pet bottle waste management options in Bauru, Brazil. *Data Brief* 33, 106355.
78. Lonca, G., Lesage, P., Majeau-Bettez, G., Bernard, S., and Margni, M. (2020). Assessing scaling effects of circular economy strategies: A case study on plastic bottle closed-loop recycling in the USA PET market. *Resour. Conserv. Recycl.* 162, 105013.
79. Boisart, C., and Maille, E. (2014). Method for recycling plastic products (World Patent No. WO 2014/079844 A1) (World Intellectual Property Organization (WIPO)).
80. Maille, E. (2017). Process of recycling mixed PET plastic articles (U.S. Patent Application Pub. No. US 2017/0114205 A1) (U.S. Patent and Trademark Office).
81. Gamerith, C., Zartl, B., Pellis, A., Guillaumot, F., Marty, A., Acero, E.H., and Guebitz, G.M. (2017). Enzymatic recovery of polyester building blocks from polymer blends. *Process Biochem* 59, 58–64.
82. Kadhum, H.J., Rajendran, K., and Murthy, G.S. (2017). Effect of solids loading on ethanol production: experimental, economic and environmental analysis. *Bioresour. Technol.* 244, 108–116.
83. Humbird, D., Mohagheghi, A., Dowe, N., and Schell, D.J. (2010). Economic impact of total solids loading on enzymatic hydrolysis of dilute acid pretreated corn stover. *Biotechnol. Prog.* 26, 1245–1251.
84. Modenbach, A.A., and Nokes, S.E. (2013). Enzymatic hydrolysis of biomass at high-solids loadings – a review. *Biomass Bioenergy* 56, 526–544.
85. Kawai, F., Kawabata, T., and Oda, M. (2019). Current knowledge on enzymatic PET degradation and its possible application to waste stream management and other fields. *Appl. Microbiol. Biotechnol.* 103, 4253–4268.
86. Ügdüler, S., Van Geem, K.M., Roosen, M., Delbeke, E.I.P., and De Meester, S. (2020). Challenges and opportunities of solvent-based additive extraction methods for plastic recycling. *Waste Manag* 104, 148–182.
87. Yang, S., Xu, H., Yan, Q., Liu, Y., Zhou, P., and Jiang, Z. (2013). A low molecular mass cutinase of *Thielavia terrestris* efficiently hydrolyzes poly(esters). *J. Ind. Microbiol. Biotechnol.* 40, 217–226.
88. Nyssölä, A., Pihlajaniemi, V., Järvinen, R., Mikander, S., Kontkanen, H., Kruus, K., Kallio, H., and Buchert, J. (2013). Screening of microbes for novel acidic cutinases and cloning and expression of an acidic cutinase from *Aspergillus niger* CBS 513.88. *Enzyme Microb. Technol.* 52, 272–278.
89. Nyssölä, A., Pihlajaniemi, V., Häkkinen, M., Kontkanen, H., Saloheimo, M., and Nakari-Setälä, T. (2014). Cloning and characterization of a novel acidic cutinase from *Sirococcus conigenus*. *Appl. Microbiol. Biotechnol.* 98, 3639–3650.
90. Johnson, E. (2016). Integrated enzyme production lowers the cost of cellulosic ethanol. *Biofuels Bioprod. Bioref.* 10, 164–174.
91. Klein-Marcuschamer, D., Oleskowicz-Popiel, P., Simmons, B.A., and Blanch, H.W. (2010). Technoeconomic analysis of biofuels: a wiki-based platform for lignocellulosic biorefineries. *Biomass Bioenergy* 34, 1914–1921.
92. Kazi, F.K., Fortman, J.A., Anex, R.P., Hsu, D.D., Aden, A., Dutta, A., and Kothandaraman, G. (2010). Techno-economic comparison of process technologies for biochemical ethanol production from corn stover. *Fuel* 89, S20–S28.
93. Le Crom, S., Schackwitz, W., Pennacchio, L., Magnuson, J.K., Culley, D.E., Collett, J.R., Martin, J., Druzhinina, I.S., Mathis, H., Monot, F., et al. (2009). Tracking the roots of cellulase hyperproduction by the fungus *Trichoderma reesei* using massively parallel DNA sequencing. *Proc. Natl. Acad. Sci. USA* 106, 16151–16156.
94. Cherry, J.R., and Fidantsef, A.L. (2003). Directed evolution of industrial enzymes: an update. *Curr. Opin. Biotechnol.* 14, 438–443.
95. Duan, X., Liu, Y., You, X., Jiang, Z., Yang, S., and Yang, S. (2017). High-level expression and characterization of a novel cutinase from malbranchea cinnamomea suitable for butyl butyrate production. *Biotechnol. Biofuels* 10, 223.
96. Duan, X., Jiang, Z., Liu, Y., Yan, Q., Xiang, M., and Yang, S. (2019). High-level expression of codon-optimized *Thielavia terrestris* cutinase suitable for ester biosynthesis and biodegradation. *Int. J. Biol. Macromol.* 135, 768–775.
97. Hong, R., Sun, Y., Su, L., Gu, L., Wang, F., and Wu, J. (2019). High-level expression of *Humicola insolens* cutinase in *pichia pastoris* without carbon starvation and its use in cotton fabric bioscouring. *J. Biotechnol.* 304, 10–15.
98. Gamerith, C., Vastano, M., Ghorbanpour, S.M., Zitzenbacher, S., Ribitsch, D., Zumstein, M.T., Sander, M., Herrero Acero, E., Pellis, A., and Guebitz, G.M. (2017). Enzymatic degradation of aromatic and aliphatic polyesters by *P. pastoris* expressed cutinase 1 from *Thermobifida cellulolytica*. *Front. Microbiol.* 8, 938.
99. Kwon, M.A., Kim, H.S., Yang, T.H., Song, B.K., and Song, J.K. (2009). High-level expression and characterization of *Fusarium solani* cutinase in *pichia pastoris*. *Protein Expr. Purif.* 68, 104–109.
100. Seman, W.M., Bakar, S.A., Bukhari, N.A., Gaspar, S.M., Othman, R., Nathan, S., Mahadi, N.M., Jahim, J., Murad, A.M., and Bakar, F.D. (2014). High level expression of *Glomerella cingulata* cutinase in dense cultures of *pichia pastoris* grown under fed-batch conditions. *J. Biotechnol.* 184, 219–228.
101. Daoud, F.B., Kaddour, S., and Sadoun, T. (2010). Adsorption of cellulase *Aspergillus niger* on a commercial activated carbon: kinetics and equilibrium studies. *Colloids Surf. B Biointerfaces* 75, 93–99.
102. Tustin, G.C., Pell, T.M., Jr., Jenkins, D.A., and Jernigan, M.T. (1995). Process for the recovery of terephthalic acid and ethylene glycol from poly(ethylene terephthalate) (US Patent No. 5413681) (U.S. Patent and Trademark Office).
103. Spychaj, T. (2005). Chemical recycling of PET: methods and products. In *Handbook of Thermoplastic Polyesters* (John Wiley & Sons), pp. 1252–1290.
104. Dye, R.F. (2001). Ethylene glycols technology. *Korean J. Chem. Eng.* 18, 571–579.
105. Shahverdi, M., Mohammadi, T., and Pak, A. (2011). Separation of ethylene glycol-water

- mixtures with composite poly(vinyl alcohol)-polypropylene membranes. *J. Appl. Polym. Sci.* **119**, 1704–1710.
106. Nik, O.G., Moheb, A., and Mohammadi, T. (2006). Separation of ethylene glycol/water mixtures using NaA zeolite membranes. *Chem. Eng. Technol.* **29**, 1340–1346.
 107. Huang, R.Y.M., Shao, P., Feng, X., and Anderson, W.A. (2002). Separation of ethylene glycol–water mixtures using sulfonated poly(ether ether ketone) pervaporation membranes: membrane relaxation and separation performance analysis. *Ind. Eng. Chem. Res.* **41**, 2957–2965.
 108. Chen, Fengrong, and Chen, Hongfang (1996). Pervaporation separation of ethylene glycol/water mixtures using crosslinked PVA/PES composite membranes. Part II. The swelling equilibrium model of the dense active layer in ethylene glycol/water mixtures. *J. Membr. Sci.* **118**, 169–176.
 109. Feng, X. (1996). Pervaporation with chitosan membranes. I. Separation of water from ethylene glycol by a chitosan/polysulfone composite membrane. *J. Membr. Sci.* **116**, 67–76.
 110. Chen, F.R., and Chen, H.F. (1996). Pervaporation separation of ethylene glycol-water mixtures using crosslinked PVA-PES composite membranes. Part I. Effects of membrane preparation conditions on pervaporation performances. *J. Membr. Sci.* **109**, 247–256.
 111. Mohammadi, T., and Akbarabadi, M. (2005). Separation of ethylene glycol solution by vacuum membrane distillation (VMD). *Desalination* **181**, 35–41.
 112. Garcia-Chavez, L.Y., Schuur, B., and de Haan, A.B. (2012). Liquid–liquid equilibrium data for mono ethylene glycol extraction from water with the new ionic liquid tetraoctyl ammonium 2-methyl-1-naphtoate as solvent. *J. Chem. Thermodyn.* **51**, 165–171.
 113. Garcia-Chavez, L.Y., Hermans, A.J., Schuur, B., and de Haan, A.B. (2012). COSMO-RS assisted solvent screening for liquid–liquid extraction of mono ethylene glycol from aqueous streams. *Sep. Purif. Technol.* **97**, 2–10.
 114. U.S. Energy Information Administration (EIA) (2018). Annual Energy Outlook 2018, Table 8, Table 16. <https://www.eia.gov/outlooks/archive/aeo18/>.
 115. Brueckner, T., Eberl, A., Heumann, S., Rabe, M., and Guebitz, G.M. (2008). Enzymatic and chemical hydrolysis of poly(ethylene terephthalate) fabrics. *J. Polym. Sci. A Polym. Chem.* **46**, 6435–6443.
 116. Wei, R., Tiso, T., Bertling, J., O'Connor, K., Blank, L.M., and Bornscheuer, U.T. (2020). Possibilities and limitations of biotechnological plastic degradation and recycling. *Nat. Catal.* **3**, 867–871.